

# Atmosphere

Volume 12 Number 3 1974

Canadian Meteorological Society  
Société Météorologique du Canada

# Atmosphere

Volume 12 Number 3 1974

## Contents

77

Numerical Experiments with the  
Pseudospectral Method in Spherical Coordinates  
*Philip E. Merilees*

97

A High Resolution Numerical Study of the Sea-Breeze Front  
*Steven Lambert*

106

The Adjustment of the Wind Field to Small Scale Topography  
In a Numerical Weather Prediction Model  
*Hubert Allard and Jacques Derome*

118

Notes and Correspondence

120

Call for Nominations – 1974 Awards

121

Book Reviews

124

Call for Papers – Ninth Annual Congress  
Andrew Thomson O.B.E. 1893–1974

---

# Numerical Experiments with the Pseudospectral Method in Spherical Coordinates

Philip E. Merilees<sup>1</sup>

University Corporation for Atmospheric Research<sup>2</sup>  
Boulder, Colorado

[Manuscript received 10 May 1974; in revised form 27 September 1974]

---

## ABSTRACT

A series of numerical experiments has been carried out to test the usefulness of the pseudospectral method for calculation of derivatives in spherical coordinates. The results indicate that the method is more accurate than a

fourth-order finite-difference scheme for the same resolution, but the two methods are of comparable efficiency. Certain aspects of the filtering problems arising in numerical models are exposed and discussed.

---

## 1 Introduction

In a recent paper (Merilees, 1973), the so-called pseudo-spectral algorithm for the approximation of derivatives in a spherical coordinate system was presented and applied to the shallow-water equations using initial conditions corresponding to a stationary solution. Those results indicated that the algorithm reproduced the stationarity of the solution to about 1 part in  $10^{12}$ . The purpose of this paper is to report on further numerical tests of the pseudo-spectral algorithm with initial conditions which lead to a time-dependent solution.

To provide an overview of the course of the experiments, a brief narrative is in order. (In the following, the term "model" refers to the shallow-water equations in advective form expressed in terms of variables defined on a latitude-longitude grid and includes the pseudospectral algorithm for the evaluation of space derivatives, a "leap frog" time differencing and various forms of filtering.) Since we use a latitude-longitude mesh, it would be necessary to use a very small time step to avoid computational instability in the polar regions. Thus, it was decided to base the maximum permissible time step for the grid length at  $60^\circ\text{N}$  and  $\text{S}$  and perform Fourier filtering of the variables from these latitudes to the poles in a way similar to that reported by Holloway *et al.* (1973, but see Merilees, 1974). This done, it was then possible to integrate the model from the stationary initial conditions with a time step of 5 min and  $\Delta\lambda = \Delta\varphi = 2\pi/64 \approx 5.6^\circ$  for about 2 days before the calculation "blew up". From the

<sup>1</sup>Present address: McGill University, Montreal, Quebec, Canada.

<sup>2</sup>The University Corporation for Atmospheric Research operates the National Center for Atmospheric Research which is sponsored by the National Science Foundation.

appearance of the instability, it was believed due to so-called nonlinear instability. Therefore, we first performed periodic (every 6 h) Fourier filtering of all 2-gridlength waves. This permitted the calculation to extend to about 4 days at which time it again “blew”. As Orszag (1971) has shown, aliasing will be eliminated if the variables are filtered with respect to 3-gridlength waves and smaller, and this was the next step. Subsequently, the model was stable for all integrations performed using initial conditions corresponding to Haurwitz waves, although we decided to perform the 3-gridlength smoother every 3 h rather than every 6 h. However, when an integration was attempted using a “real” weather map, the computation became unstable after 2 days. This instability was due to time step decoupling and was corrected with a weak time filter developed by Robert (1966) and discussed by Asselin (1972). The present version appears to be quite stable and its documentation follows.

## 2 The model

### a Equations and discretization

The governing equations are those appropriate for the description of the flow of shallow water on a sphere. They are written in advective form in terms of longitude,  $\lambda$ , and latitude,  $\varphi$ . The discretization and pseudospectral definitions of derivatives are the same as given in Merilees (1973); and centred differences are used to approximate time derivatives.

### b Fourier filtering near the poles

As stated previously, the convergence of the meridians requires an unrealistically small time step to ensure the computational stability of the explicit time-differencing scheme. Therefore, the variables are filtered from  $60^\circ\text{N}$  and  $\text{S}$  to the respective poles according to the following scheme. If  $A_{nm}$  represents a variable before filtering and  $\tilde{A}_{nm}$  the variable after filtering, then

$$\tilde{A}_{nm} = \sum_{k=-K_m}^{K_m} a_m(k) e^{ikn\Delta\lambda} \quad (1)$$

where

$$a_m(k) = \frac{1}{N} \sum_{n=1}^N A_{nm} e^{-ikn\Delta\lambda} \quad (2)$$

and  $K_m$  is the largest integer such that

$$K_m < = \frac{\cos \varphi_m}{\cos \pi/3} \cdot \frac{N}{2} \quad (3)$$

for  $|\varphi_m| > \pi/3$ . This filtering is presently applied to every variable at all time steps.

### c Periodic filtering

As stated in the narrative, it was necessary to filter wavelengths less than 3 gridlengths to ensure the stability of the calculation for periods greater than a few days. This was performed by Fourier filtering all variables in both directions, taking into account the difference between scalars and vector components.

In the present model, this filtering is performed every 3 h, although in applications with strong forcing in the small wavelengths this period may need to be shortened. Since the typical time step used is about 5 min, this filtering adds very little to the total computation.

The fact that the filtering is applied only periodically is important, because in a sense it then represents a crude closure approximation. This point will be taken up in section 6.

#### d Time filter

The model includes a time filter based on the following algorithm:

$$F^{*\tau+1} = F^{\tau-1} + \left( \frac{\partial F^*}{\partial t} \right)^\tau 2\Delta t \quad (4)$$

$$F^{\tau+1} = F^{*\tau} + \alpha(F^{*\tau+1} + F^{\tau-1} - 2F^{*\tau}) \quad (5)$$

where  $\alpha = 0.05$ . This filter strongly damps any tendency of the numerical solution to become decoupled in time.

#### e Grid sizes and time steps

Since the model requires the evaluation of Fourier transforms throughout, the resolutions tested were almost invariably chosen to be powers of 2. A time step of 5 min was sufficient to ensure the stability of calculations made with a mean free surface height of 3000 m and a resolution of  $N = 64$ ,  $M = 32$ . Experiments were also carried out with  $N = 128$ ,  $M = 64$ ,  $N = 32$ ,  $M = 16$  and  $N = 16$ ,  $M = 8$  with corresponding adjustments in the time step. (The CFL condition for the pseudospectral algorithm is  $c\Delta t \leq \Delta x/\pi$ .) The  $N = 64$ ,  $M = 32$  resolution requires about 1 sec per time step on NCAR's 6600 computer.

This completes the description of the model, except to say that a forward time differencing is used for the first extrapolation and that a parallel fast Fourier transform routine developed by David Fulker of NCAR's computing facility is used for the transform. The next section will deal with results of some experiments performed using Haurwitz wave initial conditions.

### 3 Some solutions using Haurwitz wave initial conditions

Since Phillips' (1959) paper on the integration of the primitive equations, it has become somewhat of a tradition to perform numerical tests of global models using initial conditions corresponding to so-called Haurwitz waves. The initial conditions are such that the horizontal divergence is initially zero as is its first time derivative. If the horizontal divergence remained zero, then the initial disturbance would propagate without change in shape or amplitude at the Rossby-Haurwitz phase speed. However, even with the above initial conditions, significant divergence develops and the waves do not propagate with the Rossby-Haurwitz phase speed, nor do they maintain their shape precisely. In fact, under certain circumstances, the initial disturbance may be unstable (see, for example, Hoskins, 1973).

The Haurwitz wave initial conditions are as follows. The initial flow is assumed to be nondivergent, so that  $u$  (the eastward component of wind) and

TABLE 1. Comparison of computed phase speeds of Haurwitz waves obtained by various authors.

Wave-number ( $R$ )	Authors	Numerical Scheme	Resolution	$\omega$ ( $10^{-6} \text{ sec}^{-1}$ )	$K$ ( $10^{-6} \text{ sec}^{-1}$ )	$H_0$ (km)	Length of Integration (days)	Phase Speed ( $^{\circ} \text{ day}^{-1}$ )	Amplitude Variation (%)
4	Grimmer and Shaw (1967)	Second-order	$5^{\circ}$	7.29	7.29	8	20	8.7	—
4	Phillips (1957)	Second-order	500 km	7.848	7.848	8	2	$\simeq 9$	—
4	Bourke (1972)	Spectral	Rhomboidal, Wave 10	7.29	7.29	8	4	9.2	—
4	Merilees	Pseudospectral	$360^{\circ}/32$	7.29	7.29	8	4	$9.0 \pm 0.1$	2
4	Merilees	Pseudospectral	$360^{\circ}/64$	7.29	7.29	8	4	$9.0 \pm 0.1$	2
1	Holloway <i>et al.</i> (1973)	Second-order	$\simeq 2.4^{\circ}$	7.848	7.848	8	6	$\simeq -53$	—
1	Merilees	Pseudospectral	$360^{\circ}/16$	7.848	7.848	8	6	$-50.2 \pm 9.0$	9
6	Holloway <i>et al.</i> (1973)	Second-order	$\simeq 2.4^{\circ}$	7.848	7.848	8	2	$\simeq 23$	—
6	Merilees	Pseudospectral	$360^{\circ}/64$	7.848	7.848	8	2	$23.9 \pm 0.02$	1

$v$  (the northward component of wind) may be derived from a stream function given by

$$\psi = -a^2\omega \sin \varphi + a^2K \cos^R \varphi \sin \varphi \cos R\lambda, \quad (6)$$

where  $\omega$  and  $K$  are constants and  $R$  is the wavenumber. The geopotential height field which precisely balances this initial flow is given by

$$gh = gH_0 + a^2A(\varphi) + a^2B(\varphi) \cos R\lambda + a^2D(\varphi) \cos 2R\lambda \quad (7)$$

with

$$A(\varphi) = \frac{\omega(2\Omega + \omega)}{2} c^2 + \frac{K^2}{4} c^{2R} [(R + 1)c^2 + (2R^2 - R - 2) - 2R^2c^{-2}]$$

$$B(\varphi) = \frac{2(\Omega + \omega)K}{(R + 1)(R + 2)} c^R [(R^2 + 2R + 2) - (R + 1)^2c^2]$$

$$D(\varphi) = \frac{K^2}{4} c^{2R} [(R + 1)c^2 - (R + 2)]$$

$$c = \cos \varphi.$$

The model has been integrated for various initial Haurwitz waves. In this section, we present a few representative cases and an interesting unstable case and leave a detailed comparison with other models to subsequent sections.

In Table 1 we present the phase speeds of the indicated Haurwitz waves for various resolutions and numerical schemes. The phase speeds reported here were determined by performing a spherical harmonic analysis of the vorticity field every 12 h, then averaging the 12-h phase differences over the period of the integration. This analysis was also used to determine fluctuations in phase speed and amplitude.

There are variations in phase speed and amplitude of the waves. In the case of wavenumber 4, the phase speed decreases continually throughout the integration as does the amplitude. This may explain why Grimmer and Shaw's result for average phase speed over 20 days is somewhat lower than the others. Bourke's result does seem to be somewhat high. Wavenumber 1 goes through quite rapid accelerations and decelerations with corresponding decreases and increases in amplitude. Thus, during one 12-h period it may move through 30° longitude while during the next it may move through only 20° longitude.

In general, the various models are in agreement, especially in view of the rough measurement of phase speed usually reported. As might be anticipated from the results of Holloway *et al.* (1973), the use of Fourier filtering near the poles does not cause any difficulty in the situation of strong cross-polar flow (i.e., wavenumber 1). As further evidence of the last statement, we present the results for an integration of wavenumber 1 but with a nominal free surface height of 3 km. In this case, wavenumber 1 is unstable and quite rapidly breaks down, as shown in the sequence of maps in Fig. 1. Figure 1 is a plot of the

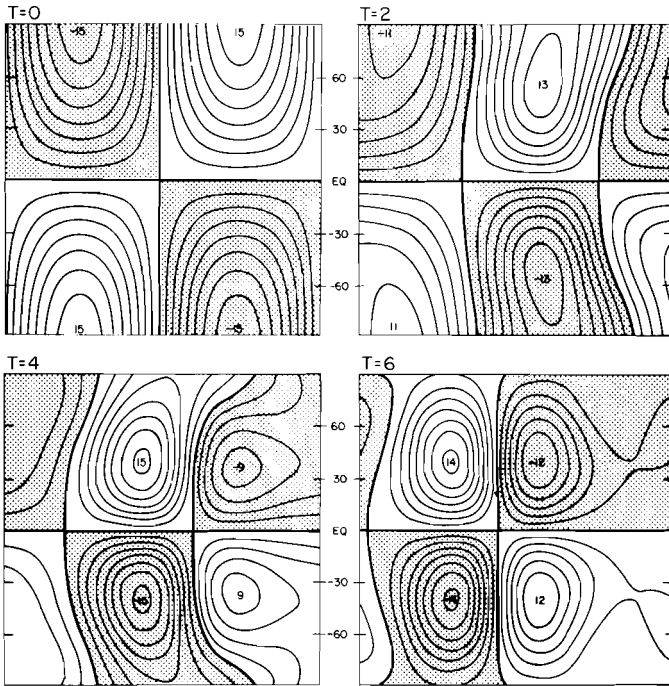


Fig. 1 Evolution of the  $v$ -component of the wind plotted on a latitude-longitude map. The initial conditions correspond to a Haurwitz wavenumber 1 with  $\omega = 7.292 \cdot 10^{-6} \text{ s}^{-1}$ ,  $K = 2.431 \cdot 10^{-6} \text{ s}^{-1}$  and the constant  $H_0$  set at 3 km. The stippled areas correspond to north winds. The contour interval is  $2 \text{ m s}^{-1}$ . Time is given in days.

$v$ -component of the wind on a map of latitude and longitude. We note that at initial time there is strong cross-polar flow ( $\approx 15 \text{ m s}^{-1}$ ). By 2 days, the maximum of the  $v$ -component has moved off the pole and by 6 days the flow has evolved into a localized vortex with the strongest flow at about  $45^\circ\text{N}$  and S. This case was also integrated using a spectral model similar to that of Bourke (1972) with virtually identical results.

#### 4 Comparisons with other models

In this section, we present the results of a detailed comparison between the pseudospectral model and other models for initial conditions corresponding to a Haurwitz wavenumber 6. These initial conditions are interesting because the flow breaks down after a couple of days, forming cut-off lows and a region of zonal easterlies at about  $50^\circ\text{N}$ . This case was used by Holloway *et al.* (1973) as a test of their numerical model and thus forms a good basis of comparison. Further, since the flow is unstable, it provides an opportunity to study the effects of the periodic filter.

We will compare the integrations for the following models: sp-15, a spectral

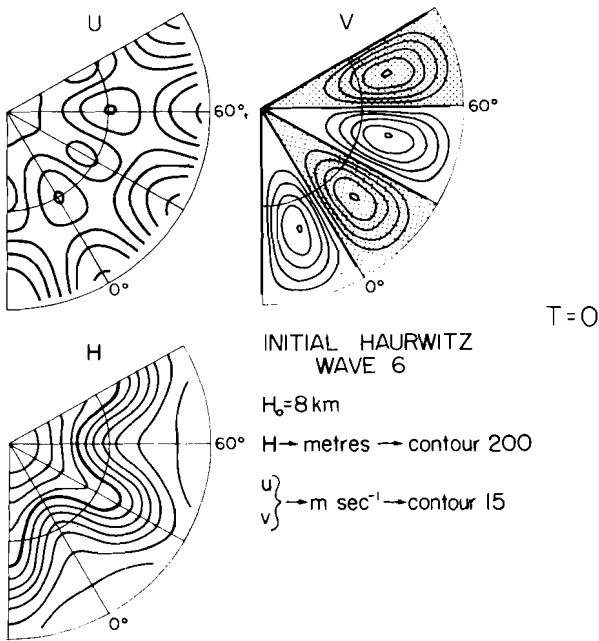


Fig. 2 Initial conditions for comparative experiments with Haurwitz wavenumber 6 plotted on a polar stereographic map of the northern hemisphere. Outer arc is the equator; inner arc is drawn with half the radius of the outer, i.e., at about  $37^\circ\text{N}$ . The heavier contour in the  $u$ - and  $v$ -fields is the zero contour with negative values stippled. The heavier contours in the height field correspond to 9000 metres. Contours are at intervals of  $15\text{ m s}^{-1}$  for the  $u$ - and  $v$ -fields, at intervals of 200 metres for the height field.

model based on spherical harmonics with a rhomboidal truncation at wave-number 15; FD4-64, the fourth-order finite difference reported by Williamson and Browning (1973) with  $64 \times 32$  gridpoints on the sphere; FD4-128, the same as FD4-64 but with  $128 \times 64$  gridpoints; and PS-64, the pseudospectral model with a  $64 \times 32$  grid.

Both the finite-difference models and the pseudospectral model employ the same polar smoother and the same periodic filter. In fact, the models are identical except for the algorithm used for the computation of derivatives. The spectral model employs the semi-implicit algorithm developed by Robert (1969) and is essentially the model developed by Bourke (1972). The initial conditions are  $\omega = 7.29 \cdot 10^{-6}\text{ sec}^{-1}$  and  $K = 7.848 \cdot 10^{-6}\text{ s}^{-1}$  while the constant  $H_0$  is  $8 \times 10^3\text{m}$ . The distributions of  $u$ ,  $v$  and  $h$  at initial time are shown in Fig. 2.

The four models are in essential agreement for about the first 3 days. In Fig. 3 are shown the geopotential height fields at 3 days. The r.m.s. differences are small, of the order of  $1\text{ m s}^{-1}$  in  $u$ ,  $v$  and about 10 m in the geopotential height field. The disturbances have propagated to the east and have developed a tilt which produces momentum transport out of the mid-latitudes as shown in the profiles of mean zonal flow (Fig. 4). It is apparent from these curves that the

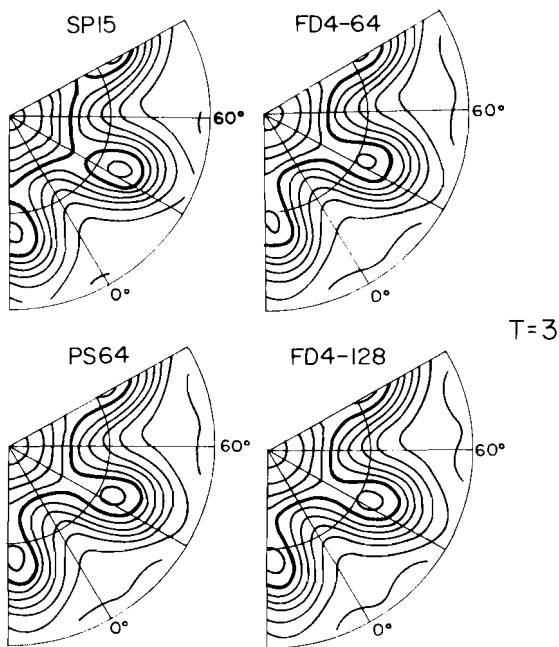


Fig. 3 Stereographic maps of the free surface height for the four models after 3 days. The outer arc is the equator; the inner arc is drawn with half the radius of the outer, i.e., at about  $37^{\circ}\text{N}$ . Contour interval is 200 m and the heavier contour has a value of 9000 m.

FD-64 model has enough resolution to handle the initial conditions reasonably well. After all, there are approximately 10 grid-points per wavelength in the 64-gridpoint case.

After about 3 days, however, the differences between the models become large, especially between the spectral model and the other three. In Fig. 5 is shown the height fields after 5 days of integration. We note the almost complete lack of the cut-off lows in the spectral model. The PS-64 and FD4-128 integration remain quite similar and there are significant differences between the latter and the FD4-64. At 6 days, (Fig. 6) and even at 8 days (Fig. 7) the PS-64 and FD4-128 models are still quite similar, although the lows are slightly deeper in the FD4-128. The spectral model has gone to a completely different state. The FD4-64 results resemble those of the FD4-128 and PS-64, but there are considerable differences in the wind fields as can be noticed from the differences in height gradient.

The mean zonal wind profiles at 6 days (Fig. 8) indicate that the FD4-64 model does not develop as strong easterlies on the north side of the cut-off lows as do the other models. The profiles of the PS-64 and FD4-128 are in close agreement, but quite different from that of the spectral model. The differences in the development of the mean zonal wind profile are the major differences in the results and may be due to the resolution in the latitudinal direction. That

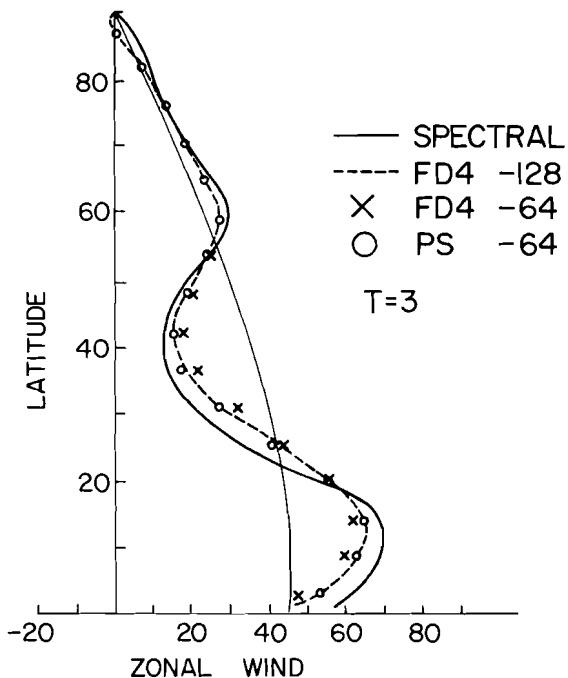


Fig. 4 Comparison of the zonal average of the  $u$ -component of the wind (in  $\text{m s}^{-1}$ ) after 3 days as a function of latitude; thin solid line is the initial profile.

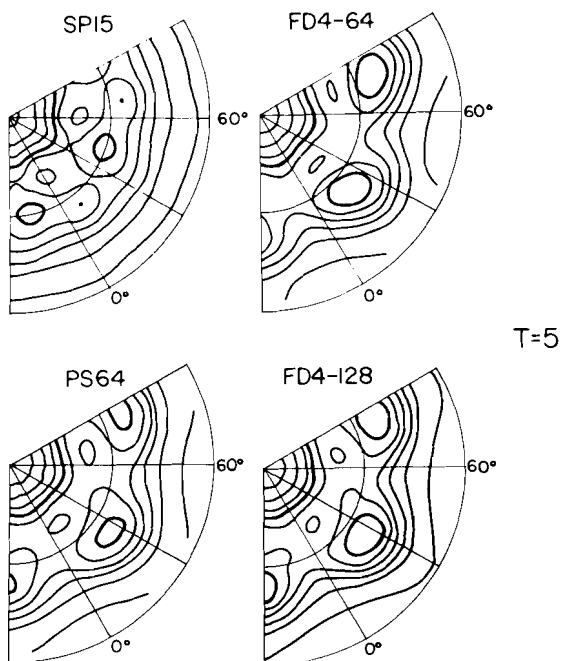


Fig. 5 Same as Fig. 3 except after 5 days.

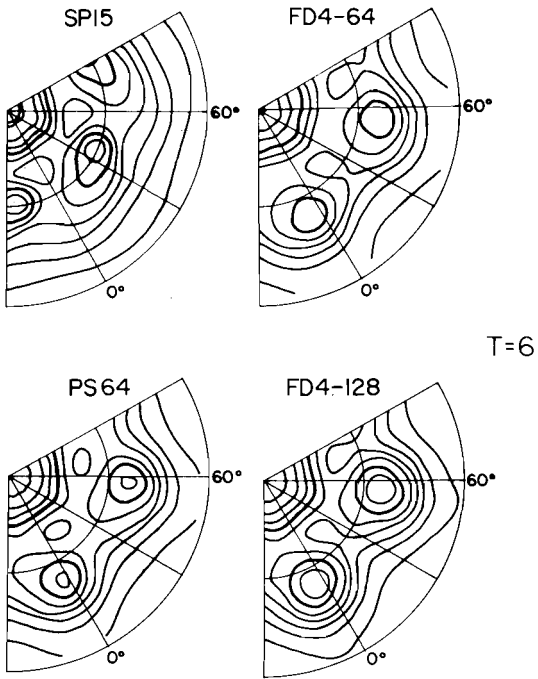


Fig. 6 Same as Fig. 3 except after 6 days.

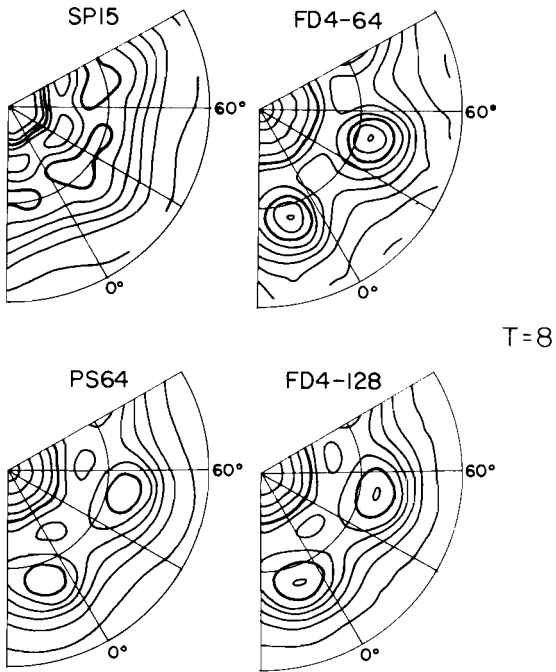


Fig. 7 Same as Fig. 3 except after 8 days.

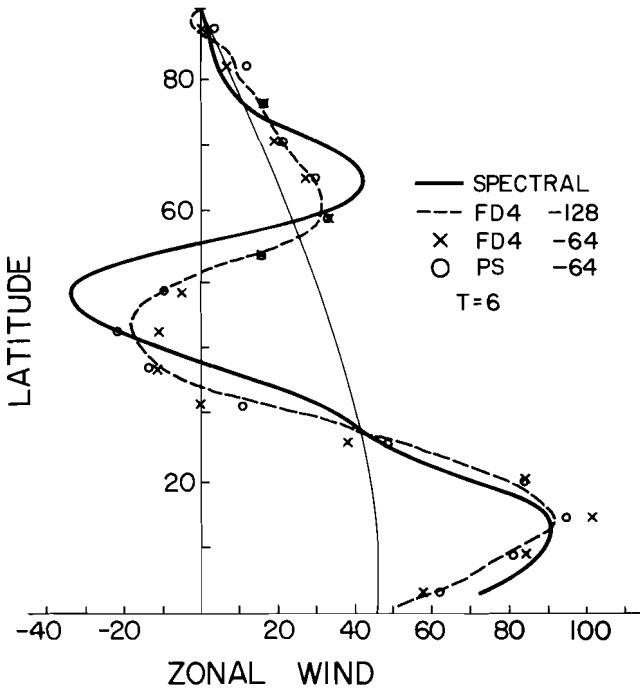


Fig. 8 Same as Fig. 4 except after 6 days.

is, the different models have different resolving power for the process of north-south momentum transport.

As a further comparison of the model results, we present trough-ridge diagrams for three latitudes (Figs. 9, 10, 11). We note that after an initial period of simple phase progression, there is a deceleration of the wave at higher latitudes and an acceleration at lower latitudes. These differences in speed are present in the initial period and actually give rise to the tilt of the wave which leads to the export of westerly momentum in the mid-latitudes. We note that the deceleration and subsequent retrogression of the waves at mid-latitudes takes place at about the same time in all models except the FD4-64 which is considerably retarded. This effect of lower resolution was also observed by Holloway *et al.* in their study of the development of similar initial conditions.

We further note the oscillations apparent in the results from the spectral model after the initial breakdown period. If one did not know that it was a spectral model, one would be tempted to invoke the words "computational mode". In a sense, these oscillations are computational since they depend on the resolution, as will be discussed in the next section.

A more quantitative comparison of the results of these integrations is provided by the r.m.s. difference between them. In Figs. 12 and 13, we present the r.m.s. difference of height and the  $v$ -components of the wind for the FD4-64 and PS-64 as compared to the FD4-128 model. These r.m.s. differences have

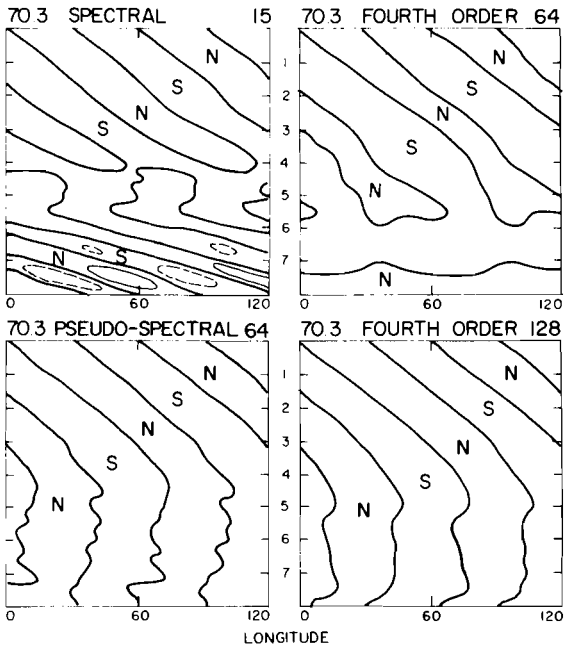


Fig. 9 Isopleths of the  $v$ -component of the wind in the longitude-time plane for the four indicated models at  $70.3^\circ\text{N}$ . Contour interval is  $15 \text{ m s}^{-1}$ . Solid lines indicate a northerly component, dashed lines a southerly component.

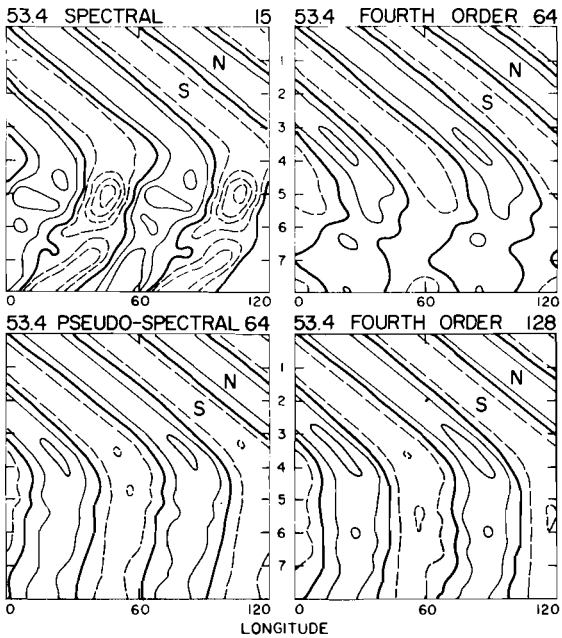


Fig. 10 Same as Fig. 8 but at  $53.4^\circ\text{N}$ .

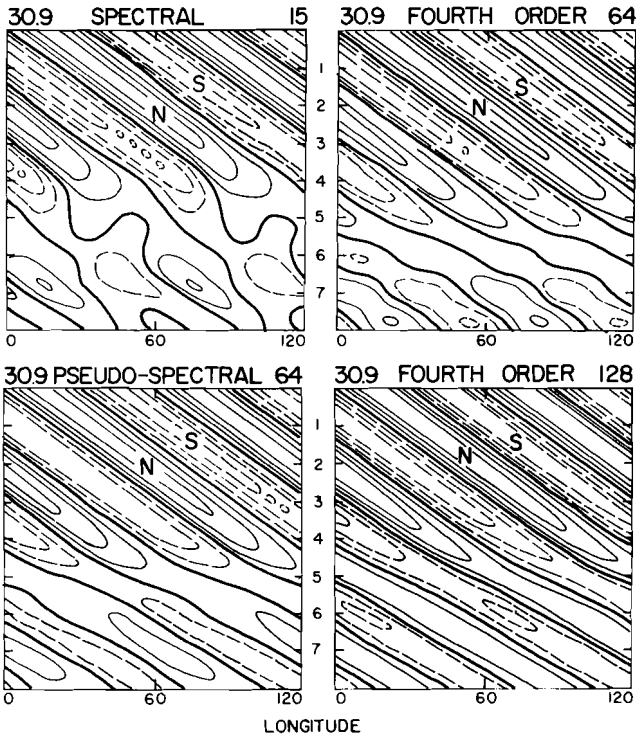


Fig. 11 Same as Fig. 8 but at 30.9° N.

not been weighted with respect to area on the sphere. The r.m.s. differences for the  $u$ -component of the wind are quite similar to the  $v$ -component and are therefore not presented. We note that these differences generally grow with time and the differences between the PS-64 and FD4-128 are invariably smaller than those between the FD4-64 and FD4-128. There is a relative minimum in the case of the FD4-64 which can only be fortuitous as the differences subsequently grow very rapidly. In the 8-day integrations, the differences between the PS-64 and FD4-128 grow to maximum values of  $6 \text{ m s}^{-1}$  in the  $v$ -component and 60 m in the height field. These differences should be compared with trough-to-ridge differences of about 600 m and meridional winds of the order of  $30 \text{ m s}^{-1}$ .

It is not clear how much of these differences is due to the existence of smaller-scale motions in the FD4-128 integration. This could be determined by performing spherical harmonic analyses and comparing the evolution of individual components, but such comparisons go beyond the scope of this report.

From the results of this section, we can fairly conclude that the PS-64 model is significantly better than the FD4-64 and quite comparable to the FD4-128 model.

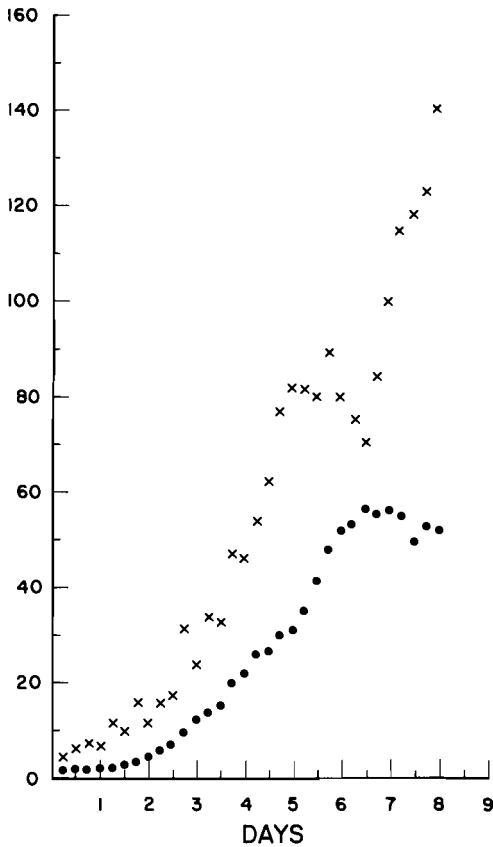


Fig. 12 r.m.s. differences in geopotential height between different models as a function of time. Ordinates given in metres. Differences between FD4-64 and FD4-128 are shown by crosses (x); between PS-64 and FD4-128 by circles (●).

### 5 The effect of resolution on the spectral model

In the previous section, it was shown that for initial conditions corresponding to a Haurwitz wavenumber 6, the four models were in good agreement for about 3 or 4 days, after which the spectral model gave results quite different from the other three. Naturally, the question arises as to whether or not the spectral model has given the correct results.

As shown below, the spectral model has not given the correct result. The reason is due to the unstable nature of the flow and the resulting cascade of enstrophy to the shorter wavelengths. Since the spectral model conserves energy and enstrophy, it must be contained in those components which the model resolution permits. Thus, if the flow is such that enstrophy should cascade to scales smaller than the model resolution, the spectral model will not permit the cascade. Subsequently, enstrophy will tend to accumulate near the shorter wavelengths permitted, then start to cascade to longer wavelengths. While the

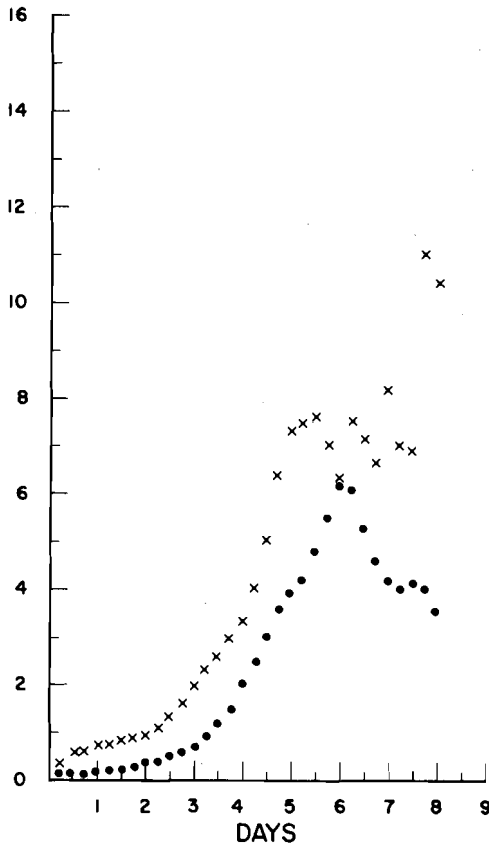


Fig. 13 Same as Fig. 11 except for the  $v$ -component of the wind and the ordinate is  $\text{m s}^{-1}$ .

spectral model will not become computationally unstable, at this point its results are definitely unphysical.

In support of these ideas, we present in Figs. 14 and 15 the results of an integration with exactly the same initial conditions as in the previous section except that the spectral model is integrated with a rhomboidal truncation at wavenumber 30. These figures should be compared with the corresponding diagrams presented in Section 4. Notice how much more closely the high-resolution model follows the PS-64 and FD4-128 than does the low-resolution model. These results confirm that the low-resolution spectral model has inadequate resolution after about 3 days.

In Tables 2 and 3, the distributions of enstrophy over longitudinal wavenumber  $M$  and over total wavenumber  $N$  are presented. Because of the initial conditions, only those wavenumbers presented are capable of participating in the exchange. We note that even at 72 h there are definite discrepancies

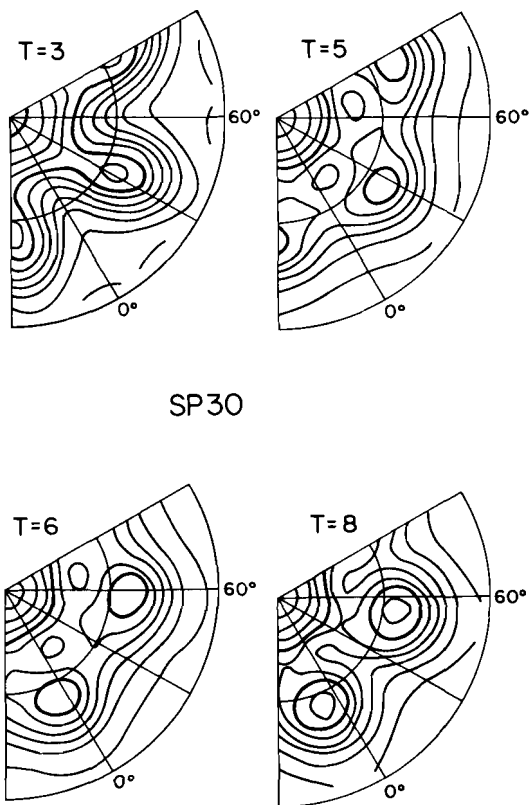


Fig. 14 Stereographic maps of the free surface height for the high resolution spectral model at various times during integration. Contour interval is 200 m and the heavier contour has a value of 9000 m.

in the large scales and a general accumulation of enstrophy in the shorter scales retained in the low-resolution integration. After 120 h, the discrepancies are generally larger and the accumulation of enstrophy near the end of the low-resolution spectrum is quite obvious. Subsequently, the low-resolution integration begins to oscillate and its development is in the direction of "equipartition" of enstrophy which appears to be the ultimate fate of nondissipative systems. At 120 h, even the high-resolution integration seems to have too much enstrophy at the end of its spectrum. However, this would have to be tested using an even higher resolution. We note that at 72 h about 1 percent of the initial enstrophy has escaped from the scales of the low-resolution model; yet there are significant differences in the scales common to both resolutions. After 120 h, roughly 10 percent of the enstrophy has escaped, which implies that less than 1 percent of energy has escaped and even less of the variance of the stream function. Thus, certainly the low-resolution model has well resolved these last two quantities; yet the time evolution is quite different.

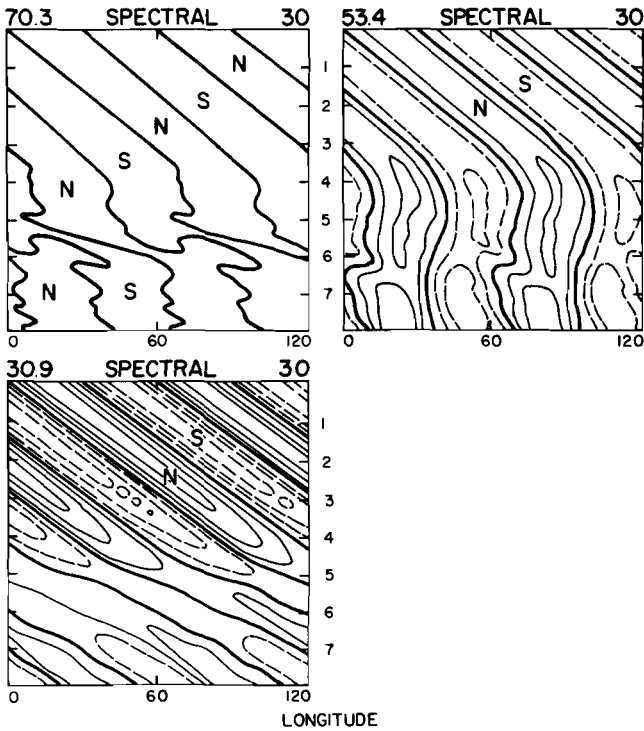


Fig. 15 Isopleths of the  $v$ -component of the wind in the longitude-time plane at three latitudes for the high-resolution spectral model. Contour interval is  $15 \text{ m s}^{-1}$ . Solid lines indicate a northerly component, dashed lines a southerly component.

## 6 Discussion of the periodic smoother

Much has been said and written about methods of numerical integration which are conservative of certain mathematical invariants of the equations describing atmospheric flow. In the previous section, a particular example was given where the property was detrimental to the solution of the equation. The reason for this is clear. Even if a set of equations has a set of invariants (say energy or enstrophy), these *conservation laws are not generally valid if the fluid is permitted to have only a finite number of degrees of freedom*. There may exist particular initial conditions which require the fluid flow to be confined to a finite number of degrees of freedom, but it would appear that such conditions would not be common and almost certainly not met in the day-to-day fluctuations of the atmosphere. It is true in certain situations that conservation of some property is valid to a high degree of approximation over a finite number of degrees of freedom. It, unfortunately, is equally true that this does not imply that the correct evolution of the flow will be simulated with such a resolution.

In the example presented in the previous section, only about 1 percent of

TABLE 2. The distributions of enstrophy ( $10^{-12} \text{ s}^{-2}$ ) over longitudinal wavenumber  $M$  and total wavenumber  $N$  for spectral models of resolutions 15 and 30 after 72 h. Only those wavenumbers capable of participating in exchange are considered.

		$M$												
		0	6	12	18	24	30							
30		124.4	986.8	11.2	7.3	2.8	2.0							
15		161.5	933.1	49.6	0	0	0							

$N$	1	3	5	7	9	11	13	15	17	19	21	23	25	27	29
30	39.1	9.8	21.6	898.6	116.2	8.7	6.0	10.3	3.8	3.6	5.3	1.1	2.5	0.6	1.0
15	40.1	15.2	47.0	786.4	142.6	26.0	20.0	40.6	14.4	4.2	2.0	1.0	3.7	1.0	0.0

		$N$														
		31	33	35	37	39	41	43	45	47	49	51	53	55	57	59
30		0.7	0.6	1.3	1.1	0.4	0.7	0.4	0.3	0.5	0.1	0.1	0.1	0.1	0.0	0.0

TABLE 3. Same as Table 2 except after 120 h.

		$M$												
		0	6	12	18	24	30							
30		665.0	416.0	51.8	25.0	13.2	8.7							
15		545.7	498.7	155.7	0	0	0							

$N$	1	3	5	7	9	11	13	15	17	19	21	23	25	27	29
30	44.0	72.2	119.8	158.7	327.2	117.2	63.2	85.6	10.2	15.7	16.7	22.9	15.5	8.9	14.1
15	44.8	85.2	120.2	94.3	247.2	206.8	84.3	35.6	83.4	37.1	96.5	54.6	0.0	10.0	0.0

		$N$														
		31	33	35	37	39	41	43	45	47	49	51	53	55	57	59
30		7.7	11.1	22.2	7.9	10.8	12.0	1.6	3.6	2.3	1.5	2.4	2.2	0.2	0.2	1.9

the energy appeared in scales unresolved by the low-resolution spectral model; yet the evolution of the flow was completely different for the two models.

The above remarks are not meant to disparage spectral models, but rather to illustrate that *all models* require some method of taking into account the effect of the unresolved scales of motion on those retained—that is, the classic closure problem. In the numerical experiments presented here, a particularly crude way of doing this was adopted, namely, periodic Fourier “chopping”. (By the term “chopping”, we mean the complete elimination of wavelengths smaller than some specified wavelength.)

From numerical experiments, we know that if we do not smooth from time to time, a model in general will accumulate enstrophy or energy in the smallest resolved scale and may “blow up”. On the other hand, if we “chop” wavelengths less than 3 grid intervals every time step, or use some conservative numerical scheme, then we will avoid “blow-ups”, but may produce nonphysical behavior of the simulation. Thus, we are led to the idea that there will exist some optimum frequency of smoothing which will produce the “best” behavior.

In the numerical experiments reported here, the only physical process operating is a cascade of enstrophy from large scales to the short scales. Thus, the periodic application of a smoother serves to dissipate the enstrophy in the shortest scales thus permitting a further cascade and preventing a reflection of enstrophy which will contaminate the larger scales.

## 7 Conclusion

It has been shown that the pseudospectral algorithm for the computation of derivatives can be used on time-dependent problems with good results. It has been demonstrated that a pseudospectral model produces more accurate results than a fourth-order scheme with equivalent resolution. Application of the algorithm does, however, take more operations, approximately 4 times as many as in a fourth-order scheme. Therefore, we have not shown that the pseudospectral algorithm is more efficient than a fourth-order scheme. However, when we compare the PS-64 with the FD4-128, it suggests that the simulations are equivalent in the scales resolved by the coarser grid. If this last statement is correct, then the algorithm would be more efficient. Further numerical experiments will be directed towards this hypothesis.

Finally, the comparisons of spectral models with the others have demonstrated a serious difficulty associated with relatively low resolution and a conservative numerical scheme. Since the amount of computation in a spectral model increases with a higher power of the number of degrees of freedom, it would appear that it is very important to investigate methods of closure for spectral models if they are to successfully compete with more traditional approaches.

## Acknowledgments

The author is grateful to his colleagues, David Williamson and Gerald Browning, for providing the fourth-order model as well as many fruitful discussions.

The spectral model code was developed by Dr. William Bourke of CSIRO, Australia, and provided to me by Dr. Roger Daley of the Dynamic Prediction Research Division of Environment Canada. Many thanks are also due Dr. Steve Hotovy who programmed the pseudospectral code.

---

## References

- ASSELIN, R.A., 1972: Frequency filter for time integrations. *Mon. Wea. Rev.*, **100**, 487–490.
- BOURKE, W., 1972: An efficient, one-level, primitive-equation spectral model. *Mon. Wea. Rev.*, **100**, 683–689.
- GRIMMER, M., and D.B. SHAW, 1967: Energy preserving integrations of the primitive equations on the sphere. *Quart. J. Roy. Meteor. Soc.*, **93**, 337–349.
- HOLLOWAY, J.L., JR., M.J. SPELMAN, and S. MANABE, 1973: Latitude-longitude grid suitable for numerical time integration of a global atmospheric model. *Mon. Wea. Rev.*, **101**, 69–78.
- HOSKINS, B.J., 1973: Stability of the Rossby-Haurwitz wave. *Quart. J. Roy. Meteor. Soc.*, **99**, 723–745.
- MERILEES, P.E., 1973: The pseudospectral approximation applied to the shallow water equations on a sphere. *Atmosphere*, **11**, 13–20.
- , 1974: On Fourier filtering near the poles. *Mon. Wea. Rev.*, **102**, 82–84.
- ORSZAG, S.A., 1971: On the elimination of aliasing in finite-difference schemes by filtering high wavenumber components. *J. Atmos. Sci.*, **28**, 1074.
- PHILLIPS, N.A., 1959: Numerical integration of the primitive equations on the hemisphere. *Mon. Wea. Rev.*, **87**, 564–570.
- ROBERT, A.J., 1966: The integration of a low order spectral form of the primitive meteorological equations. *J. Meteor. Soc. Japan, Ser. 2*, **44**, 237–245.
- , 1969: Integration of a spectral model of the atmosphere by the implicit method. *Proc. WMO/IUGG Symp. Numerical Weather Prediction*, Tokyo, Japan, November 26–December 4, 1968, Japan Meteorological Agency, Tokyo, March 1969, VII–19–VII–24.
- WILLIAMSON, D.L., and G.L. BROWNING, 1973: Comparison of grids and difference approximations for numerical weather prediction over a sphere. *J. Appl. Meteor.*, **12**, 264–274.
-

---

# A High Resolution Numerical Study of the Sea-Breeze Front

Steven Lambert<sup>1</sup>

*Atmospheric Environment Service, Montreal*

[Manuscript received 15 July 1974; in revised form 16 September 1974]

---

## ABSTRACT

The primitive equations are integrated numerically using a high resolution grid to investigate the sea-breeze front. Two cases of the sea-breeze front are

presented; the first produced in an atmosphere with a prevailing offshore flow, and the second produced in an atmosphere initially at rest.

---

## 1 Introduction

Previous investigations of the sea-breeze circulation have been carried out using relatively coarse grids for the numerical computation and as a result, many details of the circulation remained unresolved. The feature which suffered most was the sea-breeze "front" which was completely lost by some models.

The sea-breeze front was described by Defant (1951) as developing in a synoptic regime which produces offshore surface winds which oppose the development of the sea-breeze. The zone of confluence of the synoptic wind and the onshore sea-breeze marks the sea-breeze front. Its passage at a given point is marked by an abrupt windshift and a temperature drop.

A sea-breeze front can also develop in a situation where the synoptic wind is essentially calm. In this case, the sea-breeze circulation produces its own offshore wind to form a frontal zone.

The present study is an extension of the work of Neumann and Mahrer (1971) in two respects; first an increase in the spatial and temporal resolution is used and second the sea-breeze is allowed to occur in an atmosphere *not* initially at rest.

Estoque (1961, 1962) presented similar results with a model using a coarse grid and the assumption of hydrostatic equilibrium.

## 2 The Model

Following Estoque (1961), the atmosphere is partitioned into a constant flux layer extending from the surface to a height of 50 m and a layer of transition extending from 50 m to 2075 m. This upper layer contains the rows and columns of grid points used in the numerical computation.

The governing equations for the constant flux layer are:

$$\frac{\partial}{\partial z} \left( K_z \frac{\partial U}{\partial z} \right) = 0 \quad (1)$$

$$\frac{\partial}{\partial z} \left( K_z \frac{\partial \theta}{\partial z} \right) = 0 \quad (2)$$

<sup>1</sup>Present address: McGill University, Montreal, Quebec.

where  $K_z$  = vertical eddy diffusivity

$U$  = total horizontal wind

$\theta$  = potential temperature

In order to maintain continuity in the potential temperature and horizontal wind and their vertical derivatives, it is necessary to assume that the constancy of the fluxes can be extended to the first row of grid points in the transition layer. The purpose of the constant flux layer is to provide the boundary conditions for use by the prediction equations of the transition layer. Hence, it is necessary to express the values of wind and temperature at the top of the constant flux layer in terms of the values at the surface and the values at the first row of grid points in the transition layer i.e.:

$$U_h = \beta U_{h+\Delta z} + \gamma U_0 \quad (3)$$

$$\theta_h = \beta \theta_{h+\Delta z} + \gamma \theta_0 \quad (4)$$

The subscript  $h$  refers to values at the top of the constant flux layer, the subscript  $h + \Delta z$  refers to values at the first row of grid points in the transition layer, and the subscript 0 refers to values at the surface.

Since the parameters  $\beta$  and  $\gamma$  are functions of stability, it is necessary to consider both unstable and stable regimes in the constant flux layer. The Richardson Number is used as the indicator of stability. The unstable regime occurs with:

$$Ri \leq Ri_c$$

and the stable regime with:

$$Ri > Ri_c$$

where  $Ri$  = Richardson Number

$Ri_c$  = a critical Richardson Number

The Richardson Number is evaluated using:

$$Ri = \frac{g(\bar{\theta}_{h+\Delta z} - \theta_0)}{\bar{\theta}(U_{h+\Delta z} - U_0)^2} [h + \Delta z] \quad (5)$$

where  $g$  = acceleration due to gravity

$\bar{\theta}$  = average potential temperature in the constant flux layer

$h$  = height of the constant flux layer (50 m)

$\Delta z$  = vertical spacing of the grid rows in the layer of transition

The expressions for the eddy diffusivity,  $K_z$ , and the parameters  $\beta$  and  $\gamma$  were derived for the stable and unstable regimes by Estoque (1959, 1961) respectively.

For the stable regime:

$$K_z = [k_0(h + z_0)(1 + \alpha Ri)]^2 \left( \frac{U_{h+\Delta z} - U_0}{h + \Delta z} \right) \quad (6)$$

where  $k_0$  = von Karman's constant (0.4)

$z_0$  = roughness height (.02 m)

$\alpha$  = a constant (-0.03)

$$\beta = \frac{\delta_1 + \frac{\Delta z}{h + \Delta z}(\delta_1 - h\delta_2)\alpha Ri}{\delta_1 + \Delta z\delta_2} \quad (7)$$

$$\gamma = 1 - \beta \quad (8)$$

where

$$\delta_1 = \frac{1}{k_0} \log\left(\frac{h + z_0}{z_0}\right)$$

$$\delta_2 = \frac{1}{k_0(h + z_0)}$$

For the unstable regime:

$$K_z = \lambda h^2 \sqrt{\frac{g}{\theta} \left| \frac{\theta_{h+\Delta z} - \theta_0}{h + \Delta z} \right|} \quad (9)$$

where  $\lambda$  = constant (0.9)

$$\beta = 1 + 3\left(\frac{h}{h + \Delta z}\right) \left[ \left(\frac{h}{h + \Delta z}\right)^3 - 1 \right] \quad (10)$$

$$\gamma = 1 - \beta \quad (11)$$

Following McPherson (1970), the value of  $\alpha$  is taken as -0.03,  $\lambda$  as 0.9, and  $Ri_c = -0.03$ .

The equations for the transition layer are basically the two-dimensional Navier-Stokes equations for a turbulent incompressible atmosphere on the rotating earth:

$$\frac{\partial u}{\partial t} = -u \frac{\partial u}{\partial x} - w \frac{\partial u}{\partial z} - \frac{1}{\rho} \frac{\partial p}{\partial x} + fv - 2\Omega \cos\phi w + \frac{\partial}{\partial z} \left( K_z \frac{\partial u}{\partial z} \right) + K_x \frac{\partial^2 u}{\partial x^2} \quad (12)$$

$$\frac{\partial v}{\partial t} = -u \frac{\partial v}{\partial x} - w \frac{\partial v}{\partial z} - f(u - u_g) + \frac{\partial}{\partial z} \left( K_z \frac{\partial v}{\partial z} \right) + K_x \frac{\partial^2 v}{\partial x^2} \quad (13)$$

$$\frac{\partial w}{\partial t} = -u \frac{\partial w}{\partial x} - w \frac{\partial w}{\partial z} + 2\Omega \cos\phi u - \frac{1}{\rho} \frac{\partial p}{\partial z} - g + \frac{\partial}{\partial z} \left( K_z \frac{\partial w}{\partial z} \right) + K_x \frac{\partial^2 w}{\partial x^2} \quad (14)$$

$$\frac{\partial \theta}{\partial t} = -u \frac{\partial \theta}{\partial x} - w \frac{\partial \theta}{\partial z} + \frac{\partial}{\partial z} \left( K_z \frac{\partial \theta}{\partial z} \right) + K_x \frac{\partial^2 \theta}{\partial x^2} \quad (15)$$

$$0 = \frac{\partial u}{\partial x} + \frac{\partial w}{\partial z} \quad (16)$$

where  $K_x$  = horizontal eddy diffusivity  
 $f$  = Coriolis parameter  
 $\Omega$  = angular velocity of the earth  
 $u_g$  = imposed geostrophic wind  
 $\phi$  = latitude  
 $u, v, w$  = wind components.

In order to close the above system, it is necessary to include the equation of state for an ideal gas and Poisson's equation for potential temperature.

A local tangent plane co-ordinate system is used with the  $x$  axis pointing eastward, the  $y$  axis pointing northward, and the  $z$  axis pointing vertically upward. An infinitely long coastline is assumed co-incident with the  $y$  axis with the sea to the west and the land to the east.

The term  $fu_g$  in (13) allows the imposition of a large scale pressure gradient in the  $y$  direction via the steady wind  $u_g$  at the top of the transition layer.

The vertical eddy diffusivity is assumed to have an exponential decrease with height in the transition layer. McPherson's (1970) form for the height dependence is used:

$$K_z(z) = K_z(h) \exp \left\{ -m \left( \frac{z-h}{H} \right)^2 \right\} \quad (17)$$

where  $K_z(z)$  = the vertical eddy diffusivity at height  $z$

$K_z(h)$  = the vertical eddy diffusivity calculated from (6) and (9)

$m$  = constant (4.75)

$H$  = height of the top of the transition layer (2075 m.).

The value of the horizontal eddy diffusivity  $K_x$  is assumed to be constant and equal to  $500 \text{ m}^2 \text{ s}^{-1}$  in accordance with Angell, Allen and Jessup's (1971) results.

The boundary conditions at the top of the layer of transition are:

$$\frac{\partial}{\partial t}(\theta, v, u, p) = 0$$

$$w = 0$$

At the lateral boundaries the conditions are:

$$\frac{\partial}{\partial x}(\theta, u, v, p) = 0$$

$$w = 0$$

At the ground the following boundary conditions are used:

$$u = v = w = 0$$

$$T_{land} = T_0 + 16.0 \sin(15t - 110^\circ) + 4.0 \sin(30t + 75^\circ) + 0.6 \sin(45t + 66^\circ) + 0.7 \sin(60t - 115^\circ)$$

$$T_{sea} = T_0$$

$$T_{coast} = 0.5(T_{land} + T_{sea})$$

where  $t$  = time in hours measured from midnight

$T_{sea}$  = sea surface temperature

$T_{land}$  = ground temperature

$T_{coast}$  = temperature at the coastline

The form of the temperature wave used to heat the land is based on Kuo's (1968) results and gives equal land and sea temperatures at 8:00 AM.

### 3 Numerical Aspects

The equations for the layer of transition were integrated numerically on a 149 column by 29 row grid using finite differences. A forward time difference was used while the spatial terms, with the exception of the advection terms, used centered differences. The horizontal and vertical advection terms used "up-stream" differences.

Following Neumann and Mahrer (1971), the method originated by Chorin (1968) was used for solution.

A horizontal space increment of 1 km and a vertical space increment of 75 m were used. In order to maintain computational stability, a time step of 40 s was required. To control nonlinear instability, a three-point filter was applied vertically and horizontally to the potential temperature and wind fields at each time step.

### 4 Results

#### a *The sea-breeze front with an opposing offshore wind*

The initial conditions used for this integration were:

$$\begin{aligned}T_0 &= 288 \text{ K} \\u &= u_g = -3 \text{ m s}^{-1} \\v &= 0 \\ \text{surface pressure} &= 1000 \text{ mb} \\ \text{lapse rate} &= 0.0065 \text{ C m}^{-1}\end{aligned}$$

Initially, the model is integrated with equal land and sea temperatures in order to generate an Ekman Spiral in the transition layer. After this has been accomplished, the temperature wave is applied to the land. Fig. 1 shows the Ekman Spiral produced during the initialization procedure.

During the early hours of integration (time being measured from 8:00 AM), the low level offshore wind is slowly weakened. By 11:00 AM, a weak onshore flow had formed with the strongest wind occurring over the sea 4 km from the coastline. As a result, a weak sea-breeze front was present over the sea near the coast. The low level onshore flow continued to strengthen and the front began to move inland. As the front moved inland, its speed of propagation gradually diminished so that by 2:00 PM the front had become nearly stationary between six and seven kilometers inland. After 4:00 PM, the front resumed its landward motion penetrating 17 km inland by 7:00 PM. Positions of the sea-breeze front,

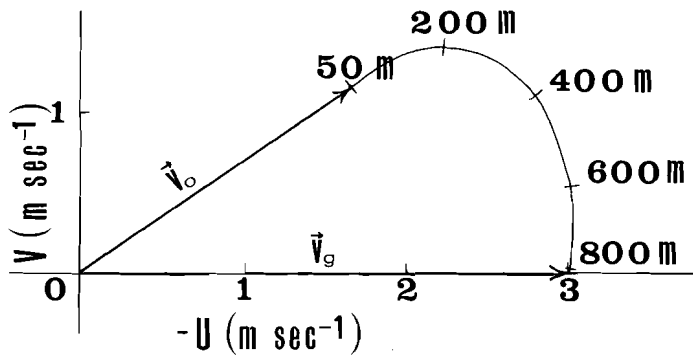


Fig. 1 Initial Ekman Spiral for the offshore wind case.  $\vec{V}_0$  is the wind at the top of the constant flux layer and  $\vec{V}_g$  is the wind at the top of the transition layer.

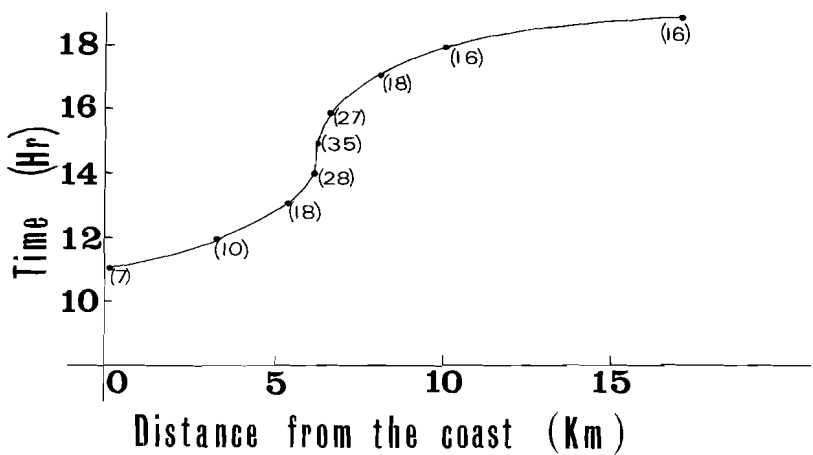


Fig. 2 Hourly positions of the sea-breeze front for the offshore wind case. Numbers in brackets are the maximum ascent in  $\text{cm s}^{-1}$  at the front.

as a function of time, are given in Fig. 2. The small figures in brackets are the strongest vertical velocities produced by the sea-breeze circulation. After 7:00 PM, rapid dissipation of the front occurred so that by 8:00 PM no onshore flow was present in the low levels.

The structure of the sea-breeze front at the time of maximum activity, 3:00 PM, is given in Fig. 3. At this time, the maximum onshore flow was  $3.0 \text{ m s}^{-1}$  with the top of the inflow layer at 450 m. An interesting feature was the strengthening of the offshore flow in the low levels just ahead of the front. As a result of the strong vertical velocity in an area which possessed a super-adiabatic lapse rate, an upward bulging of the isotherms occurred at the front producing a lowering of pressure which intensified the opposing offshore flow. Fairly strong upward vertical velocity was present above the front with the maximum of nearly  $35 \text{ cm s}^{-1}$  occurring at a height of 750 m.

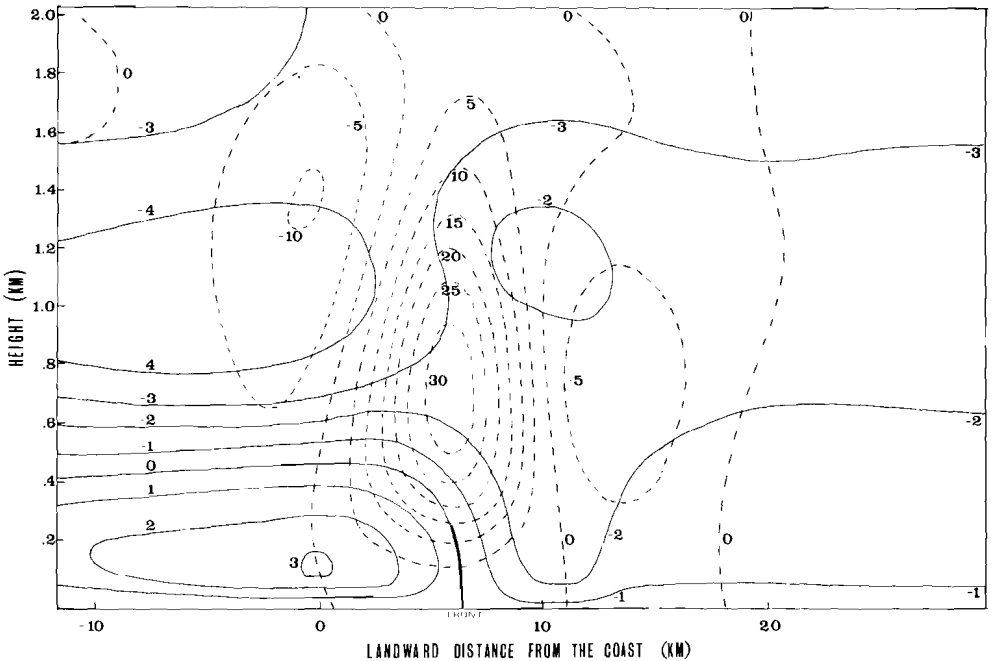


Fig. 3 The structure of the sea-breeze front at 3:00 PM for the offshore wind case. Solid lines are isopleths of the  $u$ -component in  $\text{m s}^{-1}$  and the dashed lines are isopleths of the vertical velocity in  $\text{cm s}^{-1}$ .

*b The sea-breeze front with a calm synoptic wind*

The initial conditions used for this solution were:

$$\begin{aligned}
 T_0 &= 288 \text{ K} \\
 u &= u_g = 0 \\
 v &= 0 \\
 \text{surface pressure} &= 1000 \text{ mb} \\
 \text{lapse rate} &= 0.0065 \text{ C m}^{-1}
 \end{aligned}$$

During the initial hours of integration, the sea-breeze developed at the coast-line and spread both landward and seaward and intensified. At 2:00 PM, an area of weak offshore winds had formed about 30 km inland producing a weak sea-breeze front 28 km from the coast. The front intensified quickly so that by 4:00 PM a well-developed front was present 30 km inland. Fig. 4 gives the structure of the front at 4:00 PM.

Fig. 5 shows a hodograph for a point on the coast and Fig. 6 shows a hodograph for a point 30 km inland. The coastal hodograph shows a continual intensification and veering of the wind while the inland hodograph shows a distinct wind shift with the passage of the front at 4:00 PM.

The front moved rapidly inland until it dissipated 60 km from the coast. Fig. 7 shows the frontal positions in time with the maximum vertical velocities.

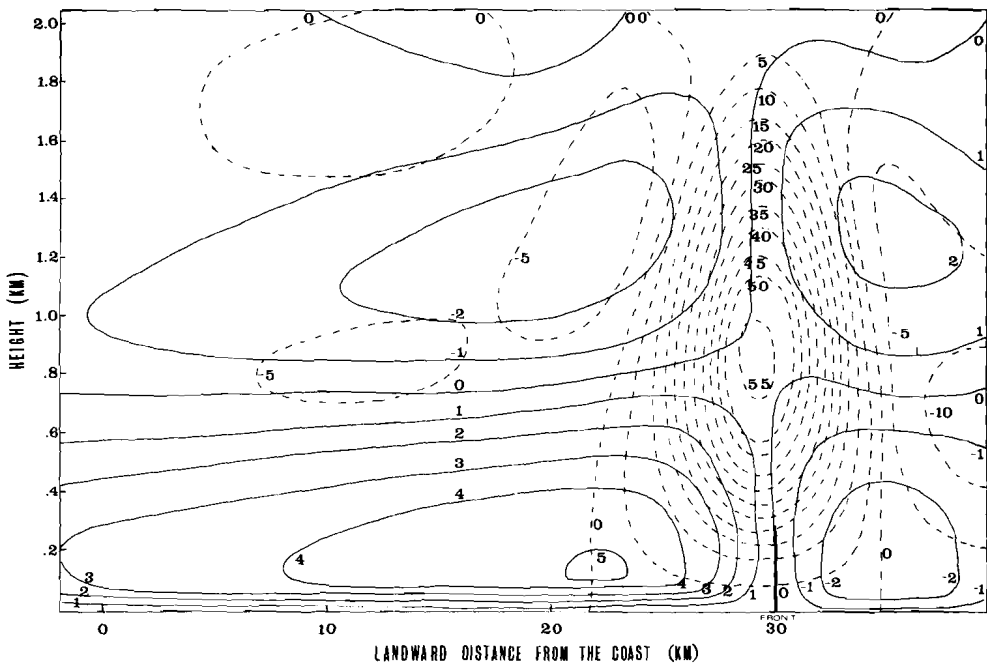


Fig. 4 The structure of the sea-breeze front at 4:00 PM for the calm synoptic wind case. Isopleths are labelled the same as in fig. 3.

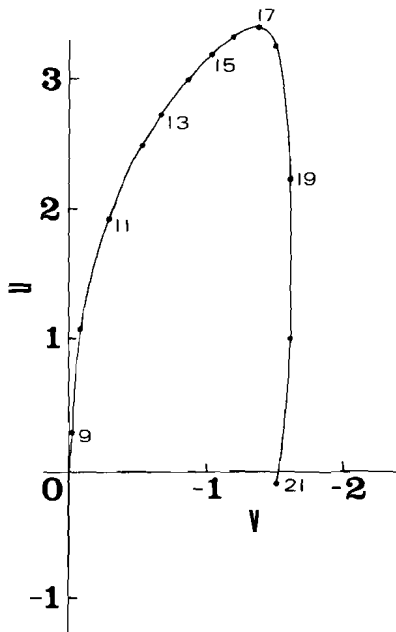


Fig. 5 Coastal hodograph for the calm synoptic wind case. The units of  $u$  and  $v$  are  $\text{m s}^{-1}$ .

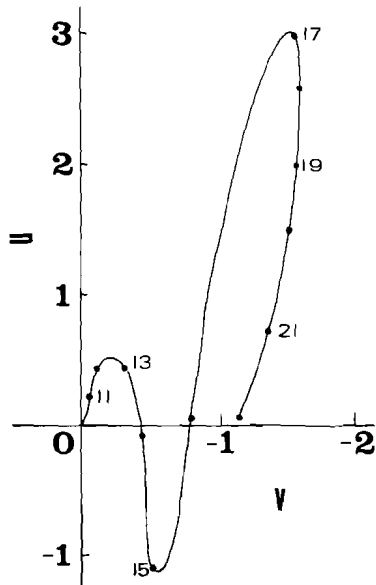


Fig. 6 Hodograph for 30 km inland for the calm synoptic wind case. The units of  $u$  and  $v$  are  $\text{m s}^{-1}$ .

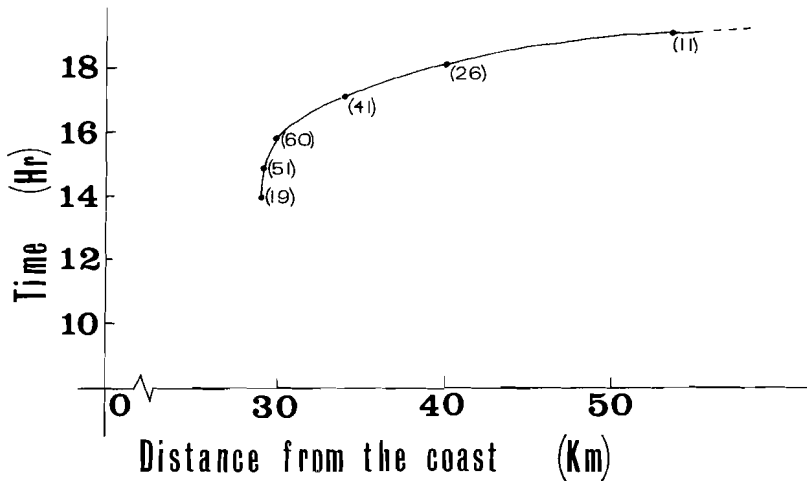


Fig. 7 Hourly positions of the sea-breeze front for the calm synoptic wind case. Numbers in brackets are the maximum ascent in  $\text{cm s}^{-1}$  at the front.

## 5 Conclusions

Observations by Lyons and Olsson (1973) of a Chicago lake breeze episode under light synoptic wind conditions show that most of the features are well-represented by the model. However, the model underforecasts the vertical velocities at the front. It was observed during numerical experimentation with the model that the vertical velocity at the front increased nearly linearly with increased horizontal resolution which indicates that a further increase in horizontal resolution would be beneficial.

## References:

- ANGELL, J. K., P. W. ALLEN, and E. A. JESSUP, 1971: Mesoscale Relative Diffusion Estimates from Tetroon Flights. *J. Appl. Met.*, **10**, 43-46.
- CHORIN, A. J., 1968: Numerical Solution of the Navier-Stokes Equations. *Math. Comput.*, **22**, 745-672.
- DEFANT, F., 1951: *Compendium of Meteorology*. Amer. Met. Soc., 658-672.
- ESTOQUE, M. A. 1959: A Preliminary Report on a Boundary-layer Experiment. *GRD Res. Notes*, **20**, AFCRC, Bedford, Mass.
- , 1961: A Theoretical Investigation of the Sea Breeze. *Quart. J. Roy. Meteor. Soc.*, **87**, 136-146.
- , 1962: The Sea Breeze as a Function of the Prevailing Synoptic Situation. *J. Atmos. Sci.*, **19**, 244-250.
- KUO, H. L., 1968: The Thermal Interaction Between the Atmosphere and the Earth and the Propagation of Diurnal Temperature Waves. *J. Atmos. Sci.*, **25**, 682-706.
- LYONS, W. A. and L. E. OLSSON, 1973: Detailed Mesometeorological Studies of Air Pollution Dispersion in the Chicago Lake Breeze. *Mon. Wea. Rev.*, **101**, 387-403.
- MCPHERSON, R. D., 1970: A Numerical Study of the Effect of a Coastal Irregularity on the Sea Breeze. *J. Appl. Met.*, **9**, 767-777.
- NEUMANN, J. and Y. MAHRER, 1971: A Theoretical Study of the Land Sea Breeze Circulation. *J. Atmos. Sci.*, **28**, 532-542.

---

# The Adjustment of the Wind Field to Small Scale Topography In a Numerical Weather Prediction Model

Hubert Allard<sup>1</sup> and Jacques Derome

*Department of Meteorology, McGill University*

[Manuscript received 26 August 1974; in revised form 21 October 1974]

---

## ABSTRACT

Numerical experiments are performed to test one reasonably economical method of producing regional forecasts. Starting with initial conditions interpolated from a 20 hour coarse grid Northern Hemisphere forecast, a fine mesh model is integrated for a further period of 4 hours over a limited area. The fine mesh is located over the north-eastern part of North America and its resolution is sufficient to re-

produce topographic features such as the St. Lawrence and Richelieu Valleys. The resulting forecast at hour 24 is then compared with the coarse mesh prediction for the same time. The comparison reveals how the horizontal and vertical components of the wind are affected by the small scale topography. In particular, the channelling effect of the main valleys is demonstrated.

---

## 1 Introduction

Most numerical weather prediction models in operational use take into account the large scale features of the main mountain barriers but lack the spatial resolution necessary to reproduce explicitly the characteristics of the ground on a subsynoptic scale. This implies, of course, that the low-level wind forecasts produced by these models are inadequate in regions where the low-level flow is strongly influenced by fine-scale topographic features. In the present study we will examine the way in which the wind field predicted by a low-resolution model can be modified so as to reflect the presence of the small scale topography following the approach suggested by Rousseau (1969). Rousseau produced a 21 hour 500 mb forecast with a barotropic primitive equation model on a hemispheric grid containing  $53 \times 57$  points. The forecast height and velocity fields were then interpolated to a higher-resolution grid covering part of Europe and the integration in time was continued for a further period of three hours with a high-resolution limited-area model. In the latter model, the earth's topography was resolved in greater detail than in the hemispheric model which implied that the initial (interpolated) data on the fine mesh were out of balance. This naturally led to the propagation of gravity waves but it was found that after three hours the height and velocity fields had reached a new balance under the influence of the topography. The adjustment between the mass and velocity fields over fine-scale orography was further

<sup>1</sup>On leave from the Atmospheric Environment Service of Canada.

examined by Rousseau (1970) using a two-dimensional baroclinic model and by Rousseau and Pham (1970) with a three-dimensional baroclinic model. In both of the latter studies the initial data supplied to the fine-mesh models were prescribed idealized conditions and adjustment periods of about two to three hours were reported. The present paper deals with similar experiments except that a fine-mesh baroclinic model is initialized from a forecast produced by a coarse-grid model. The attention will be focussed on the rate at which the flow adjusts to the new topography injected into the forecast scheme at  $t = 20$  hours and on the type of circulation which is obtained after the adjustment.

The numerical model used in this study will be presented briefly in section 2. The procedure will be explained in more detail in section 3 while the results and conclusions will follow in sections 4 and 5.

## 2 The model and procedure

The forecasts necessary for this study were done with the primitive-equation grid-point model described by Robert, Henderson and Turnbull (1972), except that the present version of the model has a surface drag mechanism of the type discussed by Shuman and Hovermale (1968). The low-resolution horizontal grid (coarse mesh) superimposed on a polar stereographic map centered at the pole has a grid length of 381 km, true at  $60^\circ\text{N}$ , so that with  $51 \times 55$  grid points it covers most of the Northern Hemisphere. The vertical coordinate of the model is given by  $\sigma = p/p_s$ , where  $p$  is the pressure and  $p_s$  is the surface pressure. The geopotential and horizontal wind components are predicted at the levels  $\sigma = 0.1, 0.3, 0.5, 0.7$  and  $0.9$  while the "vertical velocity"  $d\sigma/dt$  is carried at  $\sigma = 0.2, 0.4, 0.6$  and  $0.8$ . The coarse-mesh model uses the terrain heights given by Berkofsky and Bertoni (1955) and the drag-coefficient field of Cressman (1960).

The area covered by the fine-mesh model is delineated by the square in Fig. 1. The locations of the coarse-mesh grid points within or on the boundary of the fine-mesh area are shown by crosses. In order to resolve topographical features such as the St. Lawrence and Richelieu Valleys, a fine-mesh grid interval of 38.1 km, one-tenth of the standard one, was adopted so that the square of Fig. 1 contained  $51 \times 51$  grid points (including boundary points). The height of the terrain over the fine-mesh area was extracted from maps at every half a degree of latitude and longitude and then interpolated to the grid points. More details on the interpolation procedure can be found in Allard (1974) but it should suffice here to show the resulting contoured topographical grid-point field given in Fig. 2. It can be seen that the Laurentian Plateau (upper part of Fig. 2) and the St. Lawrence Valley (line A-B-C) are well resolved while the Richelieu Valley (B-D) creates a well defined north-south break in the Appalachians.

The values of the drag coefficient at the various grid points of the fine mesh were assigned following the method of Cressman (1960). The drag coefficient was assumed to be the sum of a first part,  $C_1 = 0.13 \times 10^{-2}$ , and a second part  $C_2$  which depends on  $h_g$ , the height of the terrain above mean sea level. Using Cressman's suggested values,  $C_2$  was assigned values which increased from 0 for



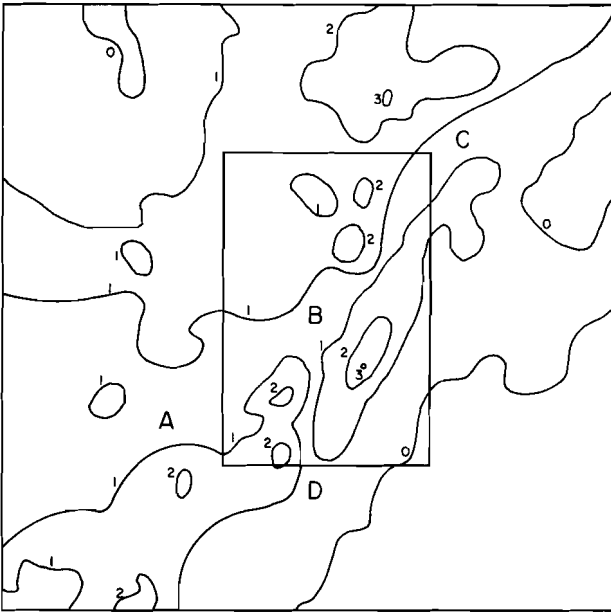


Fig. 2 Fine-mesh topographical field in thousands of feet.

For the fine-mesh forecast both horizontal wind components and the normal gradient of the surface pressure were kept fixed in time along the outer boundary of Fig. 2. Such simplified boundary conditions are of course applicable only for very short forecasts and there is little doubt that the use of time-dependent boundary conditions would constitute an improvement. It was felt, however, that in a first approach with the present model it would be justifiable to test the general procedure with time-independent boundary conditions especially since the fine-mesh integration extends only over 4 hours, over which time period the flow at the boundary can change very little. Further, in order to minimize the effect of the boundary conditions on the results to be discussed in the subsequent sections, only that part of the forecast within the inner rectangle of Fig. 2 was retained for discussion. It should be noted that the latter area is sufficiently large to include the Richelieu Valley and the major portion of the St. Lawrence Valley.

The above procedure implies that for the first 20 hours the small-scale to large-scale interactions are neglected, except for the fact that the drag coefficient used in the large-scale model increases in mountainous areas to simulate the drain of energy on the large scale by mountain-generated gravity waves (Cressman, 1960). While the approach will be assumed valid for the present study, where the small-scale orographic features have relatively small amplitudes, it should be realized that a more sophisticated approach may be required in areas of very large amplitude small-scale topography.

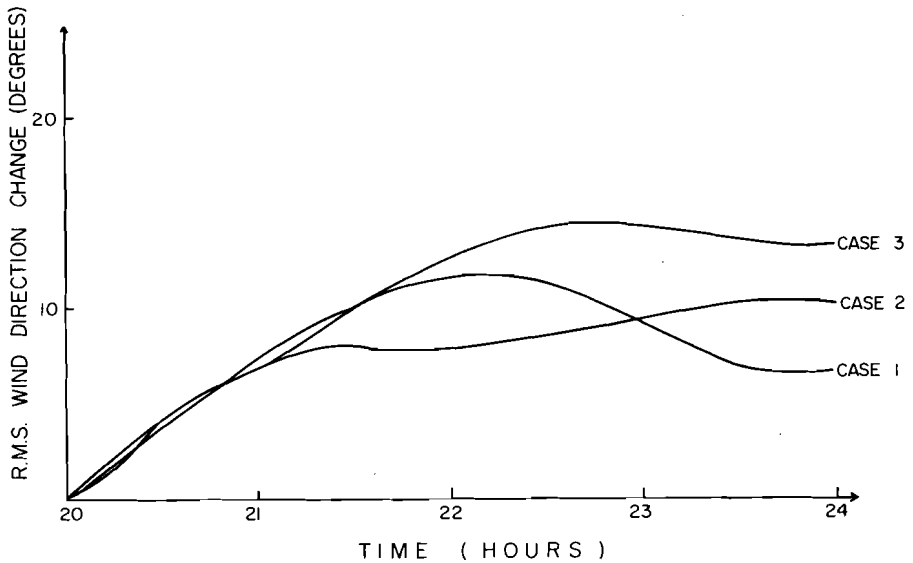


Fig. 3 Root mean square of the wind direction change (relative to  $t = 20$  hours), in degrees, as a function of time for the fine-mesh model.

### 3 The time evolution of the fine-mesh forecasts

An inspection of the fine-mesh wind-direction field displayed at regular intervals of 30 minutes (5 time steps) at  $\sigma = 0.9$  (not shown here) indicated that the latter varied continuously for the first 3 hours or so, after which definite patterns were established. To represent this time evolution quantitatively, the root mean square of the difference between the wind direction at time  $t$  and that at  $t = 20$  hours was computed at the level  $\sigma = 0.9$ . The results are presented in Fig. 3 for three different sets of initial data: CASE 1 (00Z, 26 March 1971), CASE 2 (00Z, 13 January 1973) and CASE 3 (00Z, 7 April 1973). The time evolution mentioned earlier is clearly shown for cases 2 and 3 and, to a lesser extent for case 1. We note, in particular, that after about 4 hours the high-resolution topographical influence on the wind direction is of the order of 10 degrees.

The introduction of the high-resolution topographical and drag-coefficient fields at  $t = 20$  hours can clearly be expected to lead to the generation of gravity waves. During the integration the high frequency part of the wave spectrum has been damped with time by the use of a frequency filter incorporated into the finite-difference time-stepping scheme. The latter has the form

$$F^*(t+\Delta t) = F(t-\Delta t) + 2\Delta t(\partial F/\partial t)^*,$$

$$F(t) = F^*(t) + 0.5\nu [F^*(t+\Delta t) - 2F^*(t) + F(t-\Delta t)],$$

which was first used by Robert (1966). In the above, an asterisk represents a preliminary value and the absence of an asterisk indicates the final value. For

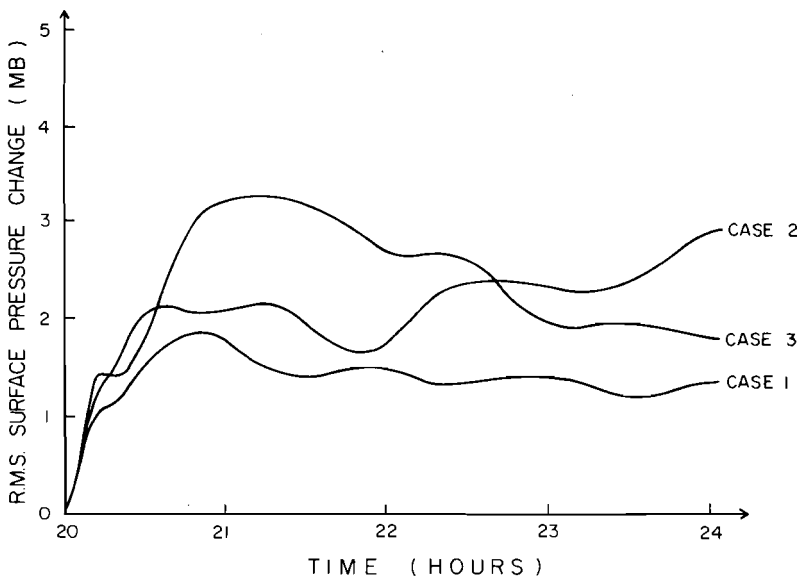


Fig. 4 Root mean square of the surface pressure change (relative to  $t = 20$  hours), in mb, as a function of time for the fine-mesh model.

the fine-mesh model  $\nu$  was set equal to 0.33. The characteristics of the filter have been discussed by Asselin (1972).

The root mean square surface pressure change (relative to  $t = 20$  hours) was also computed as a function of time in the fine-mesh model. The results, shown in Fig. 4, indicate that an important fraction of the adjustment in the surface pressure takes place within the first hour of the fine-mesh integration. This stands in contrast with the wind direction field at  $\sigma = 0.9$  (Fig. 3) which adjusts more gradually to the new topography and surface friction. In other words, the vertically integrated mass field changes appear to result mainly from relatively fast wave motions while the low-level wind-direction field adjustment seems to reflect the presence of slower oscillations, most likely of the internal gravity-wave type.

As already mentioned, Rousseau and Pham (1970) have obtained adjustment periods of about two to three hours in similar experiments. Their fine-grid primitive-equation baroclinic model was initialized by means of an idealized flow in geostrophic balance and integrated with a centered time scheme without frequency filter, using cyclic boundary conditions in the horizontal. Considering the present results shown in Figs. 3 and 4 and the fact that Rousseau and Pham seem to have estimated the adjustment period by a qualitative inspection of the predicted fields, it would appear that the two independent estimates of the adjustment period are not significantly different.

In the next section some fine-mesh forecast fields at  $t = 24$  hours will be discussed and comparisons will be made with the coarse-mesh forecast valid at the same time.

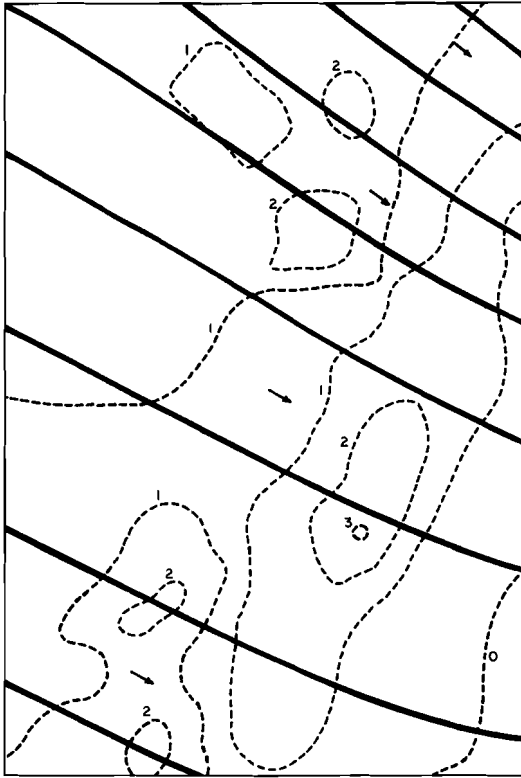


Fig. 5 Streamlines (solid lines) at  $\sigma = 0.9$  resulting from a 24-hour coarse-grid integration. The dashed lines are topographical contours at every thousand feet (used in fine-mesh model only). They will appear on all subsequent figures.

#### 4 The wind forecast after the adjustment period

We will now examine some of the forecast fields for CASE 1 (CASES 2 and 3 yielded similar results). Fig. 5 shows the streamlines at  $\sigma = 0.9$  over the inner rectangle of Fig. 2, as obtained from the 24-hour coarse-grid integration. The dashed lines are the contours of the high-resolution topography. They are presented here for reference only, since they were not used in the coarse-grid integration. It should be noticed that the case being examined is one in which the predicted low-level wind is from the northwest.

After subtracting the coarse-grid wind-direction field from the fine-mesh one valid at the same time, the difference field shown in Fig. 6 was obtained. It can be seen that the fine-mesh low-level wind rotated clockwise by up to 24 degrees in the Richelieu Valley thus becoming more nearly parallel to the north-south valley. On the other hand, a counter-clockwise rotation of up to 18 degrees was obtained near the centre of the figure, showing the channelling effect of the valley between the higher ground to the north and south.

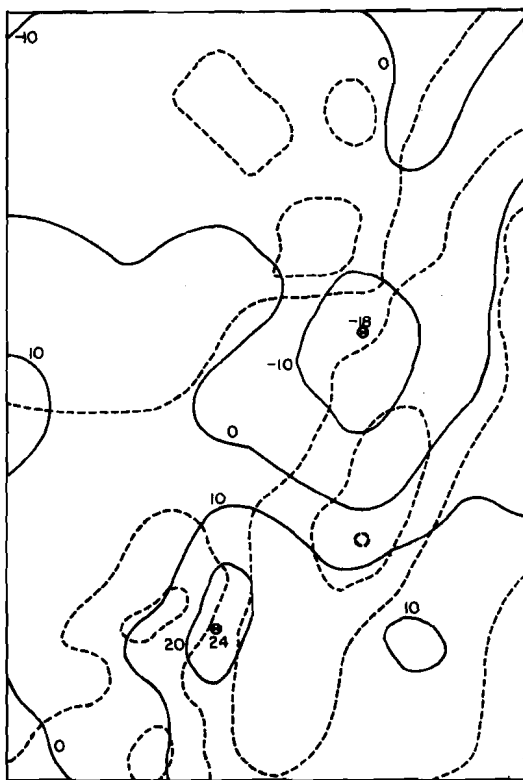


Fig. 6 Difference in wind direction (degrees) between fine- and coarse-grid forecasts at  $\sigma = 0.9$ ,  $t = 24$  hours. A positive (negative) value means that the fine-mesh wind was rotated clockwise (counterclockwise) with respect to the coarse-mesh wind.

The isotachs at  $\sigma = 0.9$  resulting from the 24-hour coarse-grid integration are presented in Fig. 7 while the difference between the coarse-grid and fine-grid wind speeds is shown in Fig. 8. It can be seen that in general the fine-mesh model yields lower wind speeds over the St. Lawrence Valley and higher wind speeds over the higher terrain, as compared to the coarse-mesh model. In other words, the air is found to accelerate as it flows over an obstacle and to decelerate as it comes to a valley.

The horizontal wind divergence field at  $\sigma = 0.9$  resulting from the fine-mesh integration is presented in Fig. 9. While there is relatively little divergence or convergence over nearly uniform terrain, areas of large divergence and convergence are found on the windward side and lee side, respectively, of the higher mountains. This is in agreement with the earlier results which showed, in particular, that on the windward side of a mountain part of the flow accelerated in going over the mountain while the rest of the flow was deflected around it.

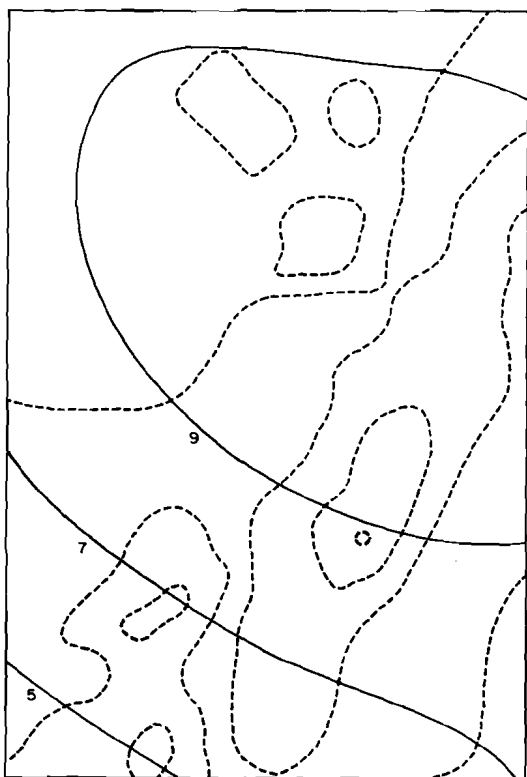


Fig. 7 Isotachs ( $\text{m s}^{-1}$ ) at  $\sigma = 0.9$  resulting from a 24-hour coarse-grid integration.

The vertical velocity  $\omega = dp/dt$  at  $\sigma = 0.9$  is shown in Fig. 10 in units of  $\mu\text{b s}^{-1}$ . Remembering that the flow is generally from the northwest it is not surprising to find the regions of negative  $\omega$  (rising motion) on the windward side of the mountainous areas and the areas of positive  $\omega$  (sinking motion) on the leeward side. Maximum values of  $\pm 5 \mu\text{b s}^{-1}$  (about  $\pm 5 \text{ cm s}^{-1}$ ) as well as maximum gradients are found near the roughest areas. Over the Atlantic (southeast corner) and the Laurentian Plateau (northwest region) the vertical motion remains very small while the air is slowly sinking on the northern side of the St. Lawrence Valley and rising on its southern side.

## 5 Conclusion

The numerical experiments indicated that a period of about three to four hours is required for a large-scale flow-pattern to adjust reasonably well to the fine-scale topography. The deflecting action of the main mountains and valleys was demonstrated and the vertical-motion field created by the air flow over the topography was discussed.

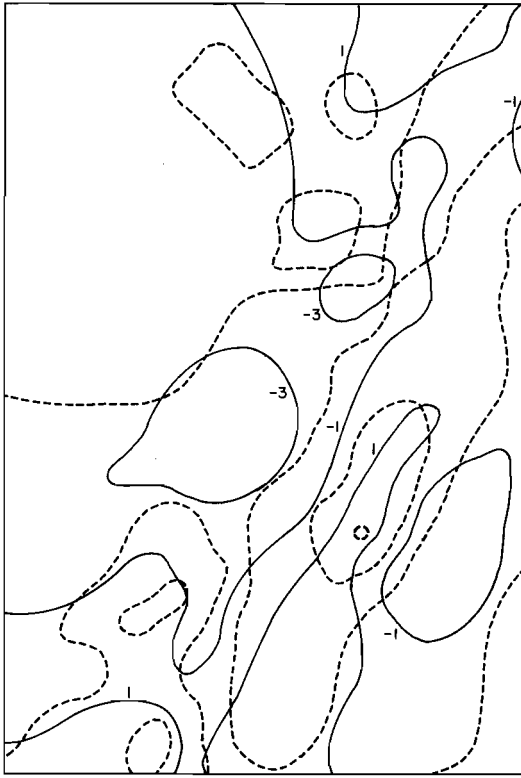


Fig. 8 Difference in wind speed at  $\sigma = 0.9$ ,  $t = 24$  hours, between fine- and coarse-grid forecasts, in  $\text{m s}^{-1}$ . A positive (negative) value means a greater (smaller) wind speed in the fine-mesh forecast.

It appears that with suitable refinements the procedure used in this study could be of practical value for regional forecasting. The present model would require approximately 20 minutes of computer time on the CDC Cyber 76 to produce a 36-hour adjusted forecast (about 10 minutes for the initialization and 32-hour coarse-grid hemispheric forecast and about 10 minutes for the 4-hour limited-area fine-mesh forecast).

One of the refinements which should be included in the model in further experiments has already been mentioned, namely, the use of time-dependent boundary conditions. A further improvement in the results could also be expected by increasing the number of "horizontal" levels of the models since the short scale features discussed in this paper are rather shallow (only minor effects on the wind field were obtained at  $\sigma = 0.7$  while the flow was essentially undisturbed at  $\sigma = 0.5$  by the small-scale topography). Finally the usefulness of the approach would be enhanced by the introduction of the moisture equation in the model since the latter could then produce quantitative forecasts of orographic clouds and precipitation rates.

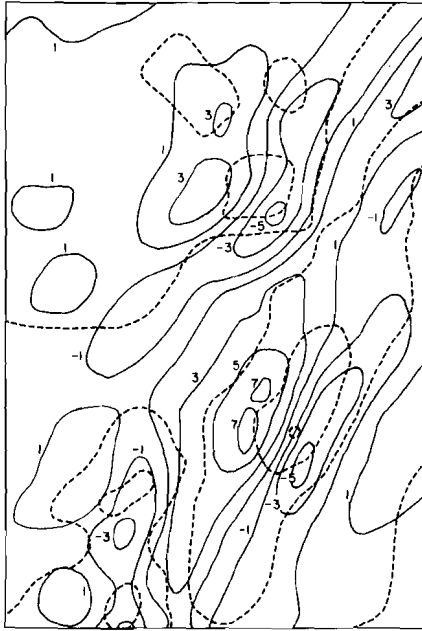


Fig. 9 The horizontal wind divergence field of the fine-mesh forecast at  $\sigma = 0.9$ ,  $t = 24$  hours, in units of  $10^{-5} \text{ s}^{-1}$ .

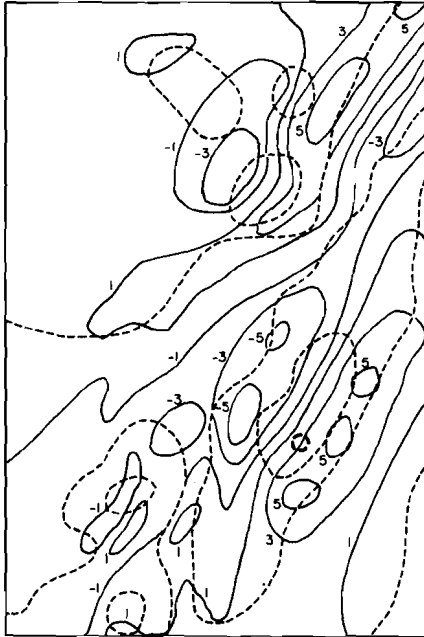


Fig. 10 The vertical motion  $\omega$  for the fine-mesh forecast at  $\sigma = 0.9$ ,  $t = 24$  hours in  $\mu\text{b s}^{-1}$ .

## Acknowledgements

The cooperation of the staff of the Dynamic Prediction Research Division of the Atmospheric Environment Service is noted with appreciation. They not only supplied the model used in the experiments but also provided guidance on the introduction of some modifications to the computer program. The second author also wishes to acknowledge the financial support received through a grant from the National Research Council of Canada.

---

## References

- ALLARD, H., 1974: Adjustment of regional wind forecasts to the topography. M.Sc. Thesis, Dept. of Meteorology, McGill University, 87 pp.
- ASSELIN, R., 1972: Frequency filter for time integrations. *Mon. Wea. Rev.*, **100**, 487–490.
- BERKOFSKY, L., and E.A. BERTONI, 1955: Mean topographic charts for the entire earth. *Bull. Amer. Meteor. Soc.*, **36**, 350–354.
- CRESSMAN, G.P., 1960: Improved terrain effects in barotropic forecasts. *Mon. Wea. Rev.*, **88**, 327–342.
- ROBERT, A.J., 1966: The integration of a low order spectral form of the primitive meteorological equations. *J. Meteor. Soc. Japan*, **44**, 237–245.
- , J. HENDERSON and C. TURNBULL, 1972: An implicit time integration scheme for baroclinic models of the atmosphere. *Mon. Wea. Rev.*, **100**, 329–335.
- ROUSSEAU, D., 1969: Expérience préliminaire à l'élaboration d'un modèle numérique de prévision régionale. *La Météorologie*, Série 5, No. 9, 5–23.
- , 1970: Etude numérique de l'action du relief sur l'atmosphère. Modèle bi-dimensionnel. *La Météorologie*. Série 5, No. 14, 1–23.
- , and H.L. PHAM, 1970: Etude numérique de l'action du relief sur l'atmosphère. Modèle tridimensionnel. *La Météorologie*, Série 5, No. 14, 25–41.
- SHUMAN, F.G. and J.B. HOVERMALE, 1968: An operational six-layer primitive equation model. *J. Appl. Meteor.*, **7**, 525–547.

---

## NOTES AND CORRESPONDENCE

---

### A NOTE ON MESO-SCALE BARRIERS TO SURFACE AIRFLOW

H. P. Wilson

*Edmonton, Alberta, 5 September 1974*

The writer first encountered the problem of anomalous winds near steeply sloping terrain soon after the Arctic Forecast Team went into operation at Edmonton in 1950. At several of the stations within our analysis area, the usual relationships between surface and gradient-level winds did not appear to hold very well. From study of thousands of surface reports and wind soundings, it was evident that although the deflection angle averaged about  $25^\circ$ , which is normal, the ratio of surface to gradient speed tended to vary with the direction of flow. For example, at Resolute, with SW flow the ratio was usually less than 0.4, but with flow with an ENE component, the ratio was frequently greater than unity, and sometimes as high as 2.0. That station is on the south coast of Cornwallis Island, which is roughly 80 kilometers in diameter, with interior elevations around 250 meters. At that time we were aware of the diagram on page 78 in Lamb's treatise, and of the promontory effect as discussed on page 240 in the Haurwitz textbook. However, we failed to recognize the significance to our problem of an introductory remark in Queney (1948) about the "cyclonic deviation of the wind flowing against a steep mountain range...."

The data on the directions of strong winds suggested the rule that they tended to be anticyclonic around islands and cyclonic around bays and straits. A similar rule appeared to be applicable to water motions around southern Greenland, Baffin Bay, and Hudson's Strait. This was taken as confirmation of our rule for wind behavior on the assumption that water moves mainly in response to wind stress.

In 1954, when we were given the task of selecting runway orientations for the original 41 Distant Early Warning sites, without the benefit of climatological data except for Cambridge Bay, that rule was used as a major consideration. The direction of strong winds predicted for Hall Beach was NNW, for Longstaff Bluff, on the east side of Foxe Basin, ESE, and for Cape Dyer, NW. These forecasts have verified very well.

Later, it was learned from experience and compilations of data that the rule could not be used when the lapse rate was neutral or nearly neutral. In such cases, the behavior was close to normal.

The exchange of correspondence between Sheppard (1956) and Scorer (1957) provided the first clue on where to look for an explanation. Sheppard asked how a surface parcel could climb over a mountain, considering that its supply of kinetic energy could easily be exhausted by work against buoyancy before reaching the level of the crest. In reply, Scorer pointed out that it could turn to the left in front of the barrier and gain the energy required from work done during the motion across the isobars toward lower pressures.

The following is a simplified version of Sheppard's derivation. Neglecting water vapor and surface friction, the energy per unit mass expended during the climb may be obtained from the relationship,  $dw/dt = -s^2z$ , where  $w$  is the vertical velocity,  $z$ , the departure from the level of rest,  $s^2 = g(\partial\theta/\partial z)/\theta$ ,  $g$ , the acceleration of gravity, and  $\theta$ , the potential temperature. Integrating,  $\Delta(w^2/2) = s^2z^2/2$ . If the source of energy for the climb is the kinetic energy of the undisturbed flow,  $U^2/2$ , the level of exhaustion is given by  $z = U/s$ .

Identifying  $U$  as the geostrophic wind, and taking surface friction into account, the level of exhaustion for a surface parcel is roughly  $0.6 U/s$ . For an isothermal condition,  $1/s$  has a value of about 50 seconds, and for  $U = 8$  meters per second, to represent mean geostrophic wind speeds, the exhaustion level is about 240 meters.

The change of kinetic energy resulting from cross-isobar motion may be described in the form,  $d(V^2/2)/dy = (u/v)du/dt + dv/dt$ , where  $V^2 = u^2 + v^2$ . Using the equations for simple horizontal motion,  $du/dt = fv$  and  $dv/dt = f(U - u)$ , where  $f$  is the Coriolis parameter,  $\Delta(V^2/2) = fU\Delta y$ . Neglecting friction so that  $V = U$  upstream, exhaustion occurs with a displacement to the right of  $U/2f$ , and  $V^2/2$  is doubled by an equivalent departure to the left. With respect to a parcel that is headed toward the center of the barrier, the width that is significant with regard to exhaustion at the right side is  $U/f$ . Taking surface friction into account, the barrier width required for stoppage on the right is about  $0.36 U/f$ . As  $1/f$  is about 3 hours, with  $U = 8$  mps,  $0.36 U/f$  is roughly 30 kilometers.

If a 10% reduction of speed in front of the barrier is regarded as a threshold for a detectable effect, it may be seen that the corresponding dimensions are  $1.0 - (0.9)^2 = 0.19$  times those required for stoppage.

These two parameters,  $U/s$  and  $U/f$ , first appeared in the literature, as a pair, in papers on lee-wave theory. A convenient reference is Corby (1954). It may be seen that both are prominent in the basic equation on page 497. Figure 3 in Queney (1948) may be regarded as an illustration of how they may combine to influence the pattern of flow over a meso-scale barrier.

Also, they may be considered in relation to the Froude ( $F$ ) and Rossby ( $Ro$ ) Numbers, as discussed on page 272 of Hess (1959). In the present context, with buoyancy as the gravitational force,  $F = U^2/h^2s^2$ , where  $h$  is the barrier height. Neglecting surface friction, with  $F \gg 1$ , the incident flow goes directly over the barrier, and with  $F \leq 1$ , it is forced to detour horizontally. The effect of the barrier becomes detectable with  $F = 25$  and increases with  $F$  decreasing toward unity.

Similarly,  $Ro$ , may be defined by  $Ro = U/bf$ , where  $b$  is the barrier width. With  $F \leq 1$ , and  $Ro \gg 1$ , the incident flow is split equally in front of the barrier, but if  $Ro \leq 1$ , practically all of it detours around to the left. The effect of the barrier is detectable with  $Ro = 5$ , and it increases as  $Ro$  decreases toward unity.

In conclusion, although our homely rule-of-thumb has been useful operationally, it seems evident that the parameters,  $U/s$  and  $U/f$ , as a pair, can be used to advantage in dealing with the problem of airflow near meso-scale barriers.

---

## References

- CORBY, G.C., 1954: The airflow over mountains: a review of the state of current knowledge, *Quart. J. Roy. Meteor. Soc.*, **80**, 491.
- HAURWITZ, B., 1941: *Dynamic Meteorology*. McGraw-Hill.
- HESS, S.L., 1959: *Introduction to Theoretical Meteorology*. Holt, Rinehart and Winston.
- LAMB, H., 1959: *Hydrodynamics*. Cambridge University Press.
- QUENEY, P., 1948: The problem of airflow over mountains: a summary of theoretical studies. *Bull. Amer. Meteor. Soc.*, **29**, 16.
- SCORER, R.S., 1957: Airflow over Mountains. *Quart. J. Roy. Meteor. Soc.*, **83**, 271.
- SHEPPARD, P.A., 1956: Airflow over Mountains. *Quart. J. Roy. Meteor. Soc.*, **82**, 528.
- 

---

## CALL FOR NOMINATIONS – 1974 AWARDS

---

Nominations are requested from members and Centres for the 1974 Society Awards to be presented at the 1975 Annual meeting. Three awards are open for competition: 1) the President's Prize for an outstanding contribution in the field of meteorology by a member of the Society; 2) the Prize in Applied Meteorology for an outstanding contribution in the field of applied meteorology by a member; and 3) the Graduate Student Prize for a contribution of special merit by a graduate student. The awards will be made on the basis of contributions during the 1974 calendar year. Nominations should reach the Corresponding Secretary not later than March 1, 1975.

Nominations are also requested from members and Centres for the award of citations to individuals or groups in Canada, who have made some outstanding contribution in helping to alleviate pollution problems or in developing environmental ethics. Nominations should reach the corresponding secretary not later than March 1, 1975.

---

## BOOK REVIEWS

---

SYNOPTIC CLIMATOLOGY. R.G. Barry and A.H. Perry. Methuen and Co. Ltd., London, 1973, 555 pp, maps, diagrams, appendix, indexes; \$37.90, cloth.

The last 30 years have seen a welcome maturity in the concepts and findings of climatology as a field of science. It was expected, therefore, that the early or middle seventies should see the publication of a few tomes summarizing the progress made in understanding processes in the atmospheric circulation. This has come to pass and volumes on concepts (Crowe), and fundamentals (Lamb and Stringer) have been reviewed elsewhere. It was therefore refreshing to hear of a publication specifically on synoptic climatology by R.G. Barry and A.H. Perry. Barry himself has been a successful textbook writer, while Perry has published a number of articles mainly on the British and Western European scenes. The high expectations anticipated of this work were not fully met, partly through an apparent hurry to put the book to press. This judgment arises from a certain imbalance in the writing style of the two authors who obviously were unable to see each other face to face as frequently as might have been desirable. There is on occasion a certain ponderousness in the writing style, and the organization of the large chapters 3, 4 and 5 tends to be more confusing than it might have been if a few more weeks of editing and rereading could have been allowed. The book, however, will be very useful as a reference, and contains an up-to-date bibliography including many from non-English sources. We would support the authors' view that the book is particularly intended for "...anyone concerned with data on the atmospheric environment..." rather than their other view that it "should fill (the) gap for advanced climatology courses at the senior undergraduate or beginning graduate level." Despite the above drawbacks, this compendium of research approaches will be a reference source for meteorologists as well as geographers.

The presentation is marred by one major weakness which was avoidable by further editing. There is, in addition to certain inaccuracies in formulae (pp. 12-59), a rather irritating repetition of anticipatory remarks to be found throughout the book. This is most noticeable between pp. 102 and 109, and on p. 109 alone three such inserts occur. Such inserts tend to induce interruptions of thought and concentration, e.g.: "the basis of harmonic analysis is discussed in Chapter 4.B (pp. 228-31) and its application to spatial problems in Chapter 4.C (pp. 263-5)." In almost all cases they are like an unexpected cold spray in a hot bath.

There is, too, a marked difference in writing style between the two authors. This is occasionally noticeable in consecutive paragraphs (paras. 2 and 3, p. 335), and more apparent from sub-section to sub-section (paras. 1 and 2, p. 319). In some parts of the book emerges an overbearing concern about subjectivity, objectivity and empiricism of results, but perhaps this is not a problem of these authors alone. In Chapter 2 occurs the cacophonous but, unfortunately, already widely accepted "parametrization"; and an occasional clumsy expression appears as in Chapter 3: "airflow ... closely related to the pressure field ... is not used as a principal element in defining the various type categories." A few meaningless and perhaps "padding" statements creep in, as:

"We now examine classifications in which the synoptic weather map is viewed in terms of airflow and the movement of pressure systems, although it should be emphasized that any attempt to separate the various approaches into rigidly distinct groups would be unrealistic. The general aims of all these studies are similar, and differences between them are essentially a matter of emphasis."

The authors state that the "basic aim of synoptic climatology ... is to relate local or regional climates to a meaningful framework—the atmospheric circulation—instead of using an arbitrary time base for assessing the average or modal types." It is a pity that they should then leave explanation of their "framework" until subsection C of Chapter 2,

and fail, until the last chapter, "Status and Prospects", to indicate that the "familiar synoptic models" used throughout the work do not pertain "to the global generality of synoptic classification methods", hence, "The regions for which such classifications have been developed are mainly, though not exclusively, in middle latitudes." It is not until the final chapter that a worthwhile attempt is made to confess that the low latitudes include a significant percentage of the circulation framework. In fact the final chapter is largely a summary of the topics treated in Chapters 3 and 5, and a catch-all section for things that were realized to have been omitted or overlooked.

The treatment is therefore unbalanced and discontinuous. It shows at times an eagerness on the part of the authors to get along with showing how much literature they have had access to. No doubt the information that will be appropriate to a student public can be tediously sought out, but at what a price of disjointedness.

For the most part, the book may be called scholarly, but what might have been a completely useful text and reference has been badly, at times confusedly, organized. This may explain the need for the numerous anticipatory inserts. Chapter 1, comprising pp. 1-7, has section A and B, with B having 2 subsections. Chapter 2 has 3 sections, 12 subsections and 8 subtitles covering pp. 8-91. Chapter 3 on Synoptic Climatological Analysis claims 4 sections, 14 subsections and 20 subtitles. Chapter 4, Statistical Methods (which might have been conveniently omitted as subordinate to specialized texts in the field of statistical methods) comprises 4 sections, 19 subsections and 8 subtitles in its 76 pages. Chapter 5 throughout its 152 pp. is worthwhile reading, even scholarly done, except for some painfully written passages between pp. 319 and 335. This chapter comprises 5 sections, 13 subsections and uses 22 subtitles. With subtitles occurring in some sections and subsections one at times gets lost as to which chapter one is in.

One misleading word usage is the subtitle of the work. The reviewers presumed that Chapter 5: "Applications" dealt with ways in which the research findings were being used in the practical and applied fields rather than how the research techniques devised were *applied* in deriving results. However, under the Section E2: *Other Applications*, a concession is made to the reader through the discussion of bioclimatology and biometeorology. The seventeen pages devoted to them deal largely with examples of research results in entomology using synoptic climatological approaches, with a few additional examples from human biometeorology—mainly studies taken from Tromp and Sargent.

One must remark on two minor features in this compendium of researchers' operational methods and their successes or failures in synoptic climatology. The first is the unabashed honesty in including the serious, recent return to studies incorporating lunar influences in weather relationships (not à la Old More's Almanack); the other is a frequent but noble admission that the basic cause of some occurrences "is still not known." Wind-shifts in the equatorial stratosphere, the question of tropospheric-stratospheric links and many other unknowns are, as the authors say, "numerous challenges (which) remain."

The work is studded with figures and other illustrations, most of which are reproductions from the original papers of the authors quoted—hence the four pages of acknowledgements. Issue can be taken with the placement of a few of the figures in relation to the text (fig. 5.10), as well as some of the reproductions (p. 61). An unaesthetic and top heavy fig. 5.23 (a) occurs on p. 341. Minor errors have slipped through such as "explicitly" (p. 7), "Panta Delgada" (p. 165), "numeral experiments" (p. 424), and some verb disagreements (p. 439). References are arranged according to chapters and chapter sections (pp. 453-528), and in the references addenda (pp. 528-530). References are also given for the Appendix with footnoted advice on the academic level of two of the five books listed.

The Appendix is not very useful. It will not help the student unfamiliar with the mathematical notions and notations, for it contains too many errors and inconsistencies, and is also far too terse to be of pedagogical value. On the other hand, people familiar with the subject matter will find the Appendix to be only an annoying appendage that the book could well have done without. On the whole, the book will be very useful, but it will be

too much to expect this edition to become the textbook of synoptic climatology. The high price will put it out of reach for most students.

S. Ivan Smith and E.R. Reinelt  
Department of Geography  
University of Alberta, Edmonton

CLIMATE CANADA. F.K. Hare and M.K. Thomas. Wiley Publishers of Canada Limited, Toronto, 1974, 256 pp., \$8.95.

This is a good and valuable book with a title which is, to put it mildly, unfortunate. Climate Canada? If it had been published by INFORMATION CANADA, or by TRANSPORT CANADA or ENVIRONMENT CANADA, then one could perhaps understand and expect to be examining a volume prepared by a government agency. But that is exactly what this book is not. For the first time we have a text book which presents a simple descriptive account of Canada's surface climates, and that is an important event. By this comment it is not intended to slight the many fine climatological publications of the Meteorological Branch, Department of Transport, and its successor the Atmospheric Environment Service. Morley Thomas' own "A Bibliography of Canadian Climate 1958-1971" (Information Canada, 1973) is an impressive compilation of reports, articles and papers totalling about 1400 items from the 15 year period 1958-1971. A previous volume (1962), which covered nearly two centuries, included about the same number. But neither bibliography listed a book like this new one.

Hare and Thomas make a fine team. The former is Professor at the University of Toronto and Director of its Institute for Environmental Studies; the latter is Director of the Meteorological Applications Branch of the Atmospheric Environment Service. Hare is the academic, the theorist who looks for synthesis and Thomas is the applied analyst who has years of experience in operational matters and an encyclopedic knowledge of Canadian climatology. The text also bears testimony to Hare's enviable, smooth command of the English language. (He once wrote a climatology book with a happy flowing title—"The Restless Atmosphere".)

The book is intended mainly for college and university students but should be useful to others like environmental scientists and engineers. It is not a book for the forecaster but rather for the geographer, biologist, soil scientist, hydrologist. There is now available another, very recent, publication which discusses the Canadian climate at a level appropriate for the professional meteorologist and climatologist. That is Vol. 11 of "World Survey of Climatology", entitled "Climates of North America" and edited by R.A. Bryson and F.K. Hare (1974).

"Climate Canada" is principally concerned with the human environment and in five parts and 14 chapters it takes the reader on an enjoyable excursion from a brief introduction to Canada's geography to climatic data processing. There is, finally, a part VI of appendices, containing very useful tables of Canadian climatic data with suitable conversion guides. In addition to the usual elements, supplementary data are given for a long list of locations, such as degree-day totals of growing and heating, freezing index, days with freezing temperature, dates of first and last frost, etc. etc., and also monthly and annual means of global radiation.

General climatology is treated in three chapters in part II, including the physical climate with a good discussion of radiation and the energy balance as well as the water regime. In this part, also, is discussed the dynamic climate and climatic change, and it gives a most satisfactory feeling to see these topics discussed in a Canadian setting. Here, as in the rest of the book, are found many original figures and tables prepared especially for the book. Also, the well-chosen plates are of Canadian scenes.

Part III describes the regional climates of Canada in two chapters and part IV turns its attention to Man and Climate. The relationships between climate and living things are discussed in a straight-forward manner with Canadian examples and the same can be said for economic activities, clothing and shelter, climate and leisure and urban climates. The

publications which may not be well known or easily accessible. In fact, each chapter of the book is followed by a list of references and of books, monographs and articles for further reading.

Finally, part V is devoted to a description of operational weather services in Canada, to sources of climatic data and, in the appendices of part VI, the data themselves.

The book gives an impression of neatness and clarity without extravagance. It is supplied with very helpful indexes, both author, geographical and subject. Hare and Thomas have performed a valuable service to Canadian meteorology and climatology by the writing of this book, in fact, to climatology in general. It will, without doubt, be widely used and appreciated. It deserves it.

Svenn Orvig  
Department of Meteorology  
McGill University, Montreal

---

### CALL FOR PAPERS – NINTH ANNUAL CONGRESS

---

The Ninth Annual Congress and Annual General Meeting of the Canadian Meteorological Society will be held at the University of British Columbia, Vancouver, B.C., 28–29–30 May 1975. The theme of the Congress will be *The Role of the Pacific in the Climate of North America*. The theme session will be composed of invited speakers. It is also planned to hold special sessions on oceanography and on forest meteorology, as well as the usual sessions on cloud physics, dynamic meteorology, micrometeorology, etc. Papers on these or any other topics are invited.

Titles and definitive abstracts (preferably less than 300 words) should reach the Program Chairman, Dr. T. Oke, Department of Geography, University of British Columbia, Vancouver, B.C. V6T 1W5 no later than *1 February, 1975*.

Information on registration, accommodation etc. will be provided in due course. The Local Arrangements Chairman is Dr. T.A. Black, Department of Soil Science, University of British Columbia, Vancouver, B.C. V6T 1W5.

---

### ANDREW THOMSON O.B.E. 1893–1974

---

With very deep regret we report the death, on 17 October 1974, in Toronto, of Dr. Andrew Thomson O.B.E., former Controller of the Canadian Meteorological Service and a founder of the Canadian Branch of the Royal Meteorological Society, the predecessor of the Canadian Meteorological Society.

Dr. Thomson's many contributions to the Canadian meteorological scene were commemorated recently in a special issue of *Atmosphere*, Vol. 11, No. 4, dedicated to him on the occasion of his 80th birthday. The enthusiastic response of the many who contributed to that issue attests to the high esteem in which he was held both here and abroad.

In a resolution passed at its meeting of 21 October 1974, the CMS Council acknowledged the large part played by Andrew Thomson in the development of meteorology in Canada and the initiatives he took to further Canadian participation in international meteorological activities. Canadian meteorology will be forever in his debt.

**Editorial policy.** *Atmosphere* is a medium for the publication of the results of original research, survey articles, essays and book reviews in all fields of atmospheric science. It is published quarterly by the CMS with the aid of a grant from the Canadian Government. Articles may be in either English or French. Contributors need not be members of the CMS nor need they be Canadian; foreign contributions are welcomed. All contributions will be subject to a critical review before acceptance. Because of space limitations articles should not exceed 16 printed pages and preferably should be shorter.

**Manuscripts** should be submitted to: the Editor, *Atmosphere*, West Isle Office Tower, 5th Floor, 2121 Trans-Canada Highway, Dorval, Quebec H9P 1J3. Three copies should be submitted, typewritten with double spacing and wide margins. Heading and sub-headings should be clearly designated. A concise, relevant and substantial abstract is required.

**Tables** should be prepared on separate sheets, each with concise headings.

**Figures** should be provided in the form of three copies of an original which should be retained by the author for later revision if required. A list of legends should be typed separately. Labelling should be made in generous size so that characters after reduction are easy to read. Line drawings should be drafted with India ink at least twice the final size on white paper or tracing cloth. Photographs (halftones) should be glossy prints at least twice the final size.

**Units.** The International System (SI) of metric units is preferred. Units should be abbreviated only if accompanied by numerals, e.g., '10 m', but 'several metres.'

**Footnotes** to the text should be avoided.

**Literature citations** should be indicated in the text by author and date. The list of references should be arranged alphabetically by author, and chronologically for each author, if necessary.

---

## RENSEIGNEMENTS POUR LES AUTEURS

---

**Politique éditoriale.** *Atmosphère* est un organe de publication de résultats de recherche originale, d'articles sommaires, d'essais et de critiques dans n'importe lequel domaine des sciences de l'atmosphère. Il est publié par la SMC à l'aide d'une subvention accordée par le gouvernement canadien. Les articles peuvent être en anglais ou en français. Il n'est pas nécessaire que les auteurs soient membre de la SMC; les contributions étrangères sont bien-venues. A cause des limitations d'espace les articles ne doivent pas dépasser 16 pages dans le format final. Tout article sera soumis à un critique indépendant avant d'être accepté.

Les **manuscrits** doivent être envoyés à : le Rédacteur, *Atmosphère*, West Isle Office Tower, 5<sup>e</sup> étage, 2121 route Trans-canadienne, Dorval, Québec H9P 1J3. Ils doivent être soumis de façon à ce qu'il soit facilement lisible après réduction du format. Le traçage des lignes doit s'effectuer au moyen d'encre de chine en doublant, au moins, le format final, le tout sur papier blanc ou sur papier à calquer et identifié adéquatement. Les photographies (demi-teintes) devraient être présentées sur épreuves glacées au double du format final.

Les **tableaux** doivent être préparés et présentés séparément accompagnés d'un titre et d'un numéro explicatifs concis.

Les **graphiques** doivent être présentés en trois copies dont les originaux devraient être conservés par l'auteur au cas où ils seraient nécessaire de les reviser. Une liste des légendes des graphiques doit être dactylographiée séparément. L'étiquetage doit être de grand format de façon à ce qu'il soit facilement lisible après réduction du format. Le traçage des lignes doit s'effectuer au moyen d'encre de chine en doublant, au moins, le format final, le tout sur papier blanc ou sur papier à calquer et identifié adéquatement. Les photographies (demi-teintes) devraient être présentées sur épreuves glacées au double du format final.

Les **unités.** Le Système International (SI) d'unités métriques est préférable. Les unités devraient être abrégées seulement lorsqu'elles sont accompagnées de nombres, ex: "10m", mais "plusieurs mètres".

Les **notes de renvoi** au texte doivent être évitées.

Les **citations littéraires** doivent être indiquées dans le texte selon l'auteur et la date. La liste des références doit être présentée dans l'ordre alphabétique, par auteur et, si nécessaire, dans l'ordre chronologique pour chaque auteur.

---

## The Canadian Meteorological Society/La Société Météorologique du Canada

---

The Canadian Meteorological Society came into being on January 1, 1967, replacing the Canadian Branch of the Royal Meteorological Society, which had been established in 1940. The Society exists for the advancement of Meteorology, and membership is open to persons and organizations having an interest in Meteorology. At nine local centres of the Society, meetings are held on subjects of meteorological interest. *Atmosphere* as the scientific journal of the CMS is distributed free to all members. Each spring an annual congress is convened to serve as the National Meteorological Congress.

Correspondence regarding Society affairs should be directed to the Corresponding Secretary, Canadian Meteorological Society, c/o Dept. of Meteorology, McGill University, P.O. Box 6070, Montreal, P.Q. H3C 3G1

There are three types of membership – Member, Student Member and Sustaining Member. For 1974 the dues are \$15.00, \$5.00 and \$50.00 (min.), respectively. The annual Institutional subscription rate for *Atmosphere* is \$10.00.

Correspondence relating to CMS membership or to institutional subscriptions should be directed to the University of Toronto Press, Journals Department, 5201 Dufferin St., Downsview, Ontario, Canada, M3H 5Y8. Cheques should be made payable to the University of Toronto Press.

---

La Société météorologique du Canada a été fondée le 1<sup>er</sup> janvier 1967, en remplacement de la Division canadienne de la Société royale de météorologie, établie en 1940. Cette société existe pour le progrès de la météorologie et toute personne ou organisation qui s'intéresse à la météorologie peut en faire partie. Aux neuf centres locaux de la Société, on peut y faire des conférences sur divers sujets d'intérêt météorologique. *Atmosphere*, la revue scientifique de la SMC, est distribuée gratuitement à tous les membres. A chaque printemps, la Société organise un congrès qui sert de Congrès national de météorologie.

Toute correspondance concernant les activités de la Société devrait être adressée au Secrétaire-correspondant, Société météorologique du Canada, Département de Météorologie, l'Université McGill, C.P. 6070, Montréal, P.Q. H3C 3G1

Il y a trois types de membres: Membre, Membre-étudiant, et Membre de soutien. La cotisation est, pour 1974, de \$15.00, \$5.00 et \$50.00 (min.) respectivement. Les Institutions peuvent souscrire à *Atmosphere* au coût de \$10.00 par année.

La correspondance concernant les souscriptions au SMC ou les souscriptions des institutions doit être envoyée aux Presses de l'Université de Toronto, Département des périodiques, 5201 Dufferin St., Downsview, Ontario, Canada, M3H 5T8. Les chèques doivent être payables aux Presses de l'Université de Toronto.

---

### Council/Conseil d'Administration: 1974-75

---

<i>President/Président</i>	– A.J. Robert	<i>Councillors-at-large/Conseillers</i>
<i>Vice-President/Vice-Président</i>	– P.E. Merilees	A.F. McQuarrie
<i>Past President/Président sortant</i>	– W.F. Hitschfeld	R.H. Silversides
<i>Corresponding Secretary/Secrétaire-correspondant</i>	– H.G. Leighton	C.V. Wilson
<i>Treasurer/Trésorier</i>	– I.N. Yacowar	<i>Chairmen of Local Centres/Présidents des centres</i>
<i>Recording Secretary/Secrétaire d'assemblée</i>	– R. Asselin	

#### ATMOSPHERE

<i>Editorial Committee/Comité de rédaction</i>		
<i>Editor/Rédacteur</i>	I.D. Rutherford	
<i>Associate Editors/Rédacteurs Associés</i>	C. East	D.N. McMullen
	J.B. Gregory	P.E. Merilees
	W. Gutzman	R.R. Rogers
	R. List	V.R. Turner
	C.L. Mateer	E.J. Truhlar
	G.A. McBean	E. Vowinckel
<i>Sustaining Member/Membre de soutien</i>		Air Canada